

WILCOX GROUP FACIES AND SYNDEPOSITIONAL SALT  
DOME GROWTH, SOUTHERN EAST TEXAS BASIN

S. J. Seni and G. E. Fogg

Assisted by

E. Bramson, D. Dann, S. Ghazi, S. Lovell, and J. Smith

## CONTENTS

ABSTRACT

INTRODUCTION

METHODOLOGY

Limitations of study  
Terminology

DEPOSITIONAL SYSTEMS

Regional Stratigraphic Framework  
Fluvial System  
    Channel facies  
    Interchannel facies  
Delta System  
    Deltaic facies  
    Saline anomalies in deltaic facies  
Modern Analogue

LITHOFACIES FRAMEWORK AND SALT TECTONIC ACTIVITY  
Oakwood Dome

RECOMMENDATIONS

SUMMARY AND CONCLUSIONS

ACKNOWLEDGMENTS

REFERENCES

APPENDIX 1

APPENDIX 2

APPENDIX 3

APPENDIX 4

## FIGURES

1. Index map showing study area and structural features.
2. Cross section showing relationship of study area to regional depositional systems framework.
3. Map of study area showing well control, cross sections, and dome locations.
4. Hydraulic conductivities and resistivities from TOH-2A and TOH-2A0.
5. SP and resistivity log illustrating Eocene stratigraphy and facies.
6. Facies map, middle one-third Wilcox Group.
7. Facies map, lower one-third Wilcox Group.
8. SP and resistivity log showing characteristic patterns of channel facies.
9. Dip-oriented cross section through channel facies.
10. Strike-oriented cross section through channel and interchannel facies.
11. Core of channel lag conglomerate.
12. SP and resistivity log showing characteristic patterns of interchannel facies.
13. Dip-oriented cross section through interchannel facies.
14. Facies map, upper one-third Wilcox Group and contour map of lignite beds.
15. Dip-oriented cross section showing deltaic facies in southern part of study area.
16. SP, Gamma, and resistivity log showing characteristic patterns of channel, interchannel, and deltaic facies.
17. SP and resistivity logs showing ground water anomaly around Oakwood Dome.
18. Histograms of relief and percent of overdome area covered by sand.
19. Map of northeastern Texas coast showing location of shallow domes and surficial sand.

20. Map of domal uplifts and rim synclines.
21. Fence diagram showing Wilcox lithofacies.
22. Cross section, Bethel Dome area.
23. Map Oakwood Dome area showing location of drill holes, core and cross sections.
24. Isopach map, study area showing regional thickness trends and thin areas over domes.
25. SP and resistivity log showing characteristic over dome thinning.
26. Isopach map, Oakwood Dome area.
27. Lithofacies cross section, Oakwood Dome area.
28. Cross section, Oakwood Dome area.

#### TABLES

1. East Texas salt domes and variations in Wilcox Group.

#### APPENDICES

1. Well name and identification number.
2. Core description, lithologic log, and grain size data from LETCO TOH-2A and geophysical data from LETCO TOH-2A0.
3. Lithofacies maps of net and percentage sandstone greater than 20  $\mu$ -m.
4. Compressed cross sections of lithofacies data.

## FIGURE CAPTIONS

- Figure 1. Study area and regional setting. Major features include Interior Mesozoic Salt Dome Basins (East Texas and North Louisiana), Gulf Coast Salt Dome Basins, Sabine Uplift faults, Mississippi River and delta system, and local drainage. Map modified from Anderson and others (1963).
- Figure 2. Relationship of study area to component facies of the Mt. Pleasant Fluvial System and Rockdale Delta System (after Fisher and McGowen, 1967).
- Figure 3. Location map of study area including salt domes, subsurface data base, and cross sections. Drill holes, core, and cross section around Oakwood Salt Dome are located in Figure 15.
- Figure 4. Hydraulic conductivities, core permeabilities and induction resistivity log from Law Engineering Testing Company (LETCO) TOH-2A0 (core) and TOH-2A (induction log). Hydraulic conductivities measured from pump tests and core permeabilities of highly resistive sandstones (greater than  $20 \Omega\text{-m}$ ) are from one to three orders of magnitude greater than sandstones with resistivities less than  $20 \Omega\text{-m}$  (after Fogg, 1980, in press).
- Figure 5. Geophysical log from McBee #1 Holley (KA-38-25-502) showing typical log pattern and depositional environments of Eocene Strata in the study area.
- Figure 6. Dip-oriented trends of net sandstone greater than  $20 \Omega\text{-m}$  outline channel facies for the middle one-third of the Wilcox. The contour of 100 ft net sandstone greater than  $20 \Omega\text{-m}$  outlines the channel facies; arrows show the thickest accumulations of sandstone and the main axes of sediment transport. Dip-oriented trends continue across the study area

as fluvial systems fed the main Wilcox deltaic depocenters 80 to 160 km (50 to 100 mi) south of the study area.

Figure 7. The fluvial-deltaic facies boundary for the lower one-third of the Wilcox is marked by the change from dip to strike orientation in the trends of net sandstone greater than 20 m. The contour of 100 ft net sandstone greater than 20 m outlines the channel facies arrows show thickest accumulations of sandstone and the main axes of sediment transport. A small, thin delta lobe occurred in Leon County during early Wilcox-time. The whole study area is underlain by a very thin progradational deltaic sequence but only in the southern part of the study area does the deltaic section thicken enough to be recognized on net sandstone maps.

Figure 8. Geophysical log from Huggins, Lane, and Cove #1 Cove (AA-38-11-623) illustrating the dominance of fluvial channel sandstones in central Anderson County. Channel sandstones are characterized by upward-fining sequences and by resistivities greater than 20 m.

Figure 9. Dip-oriented cross section Z-Z' located in Figure 3. Cross section is positioned within a major alluvial sandstone belt in Anderson and northern Houston counties. Channel complexes are dominated by sandrich upward-fining sequences. Most of the sandstone is concentrated in the central one-third of the Wilcox section.

Figure 10. Strike-oriented cross section W-W' located in Figure 3. Cross section is oriented East-West across the trend of two thick net sandstone belts associated with a major channel system in Anderson county. The eastern belt is thickest and it occurs throughout the Wilcox section. The thinner (less sandy) western belt is developed best in the upper part of the Wilcox (see fig. 13 for the fluvial sandstone trends in the upper one-third of the Wilcox). Sandstone may pinch out very rapidly

in a strike direction (East-West) as between AA-38-11-604 and AA-38-12-103. This rapid change in a strike direction contrasts with the relatively greater sandstone continuity in a dip direction (fig. 9).

Figure 11. Photograph of basal channel lag (950 ft-depth) in LETCO TOH-2A0. Scale is cm on left and in. on right. Mudclast pebbles are floating in a fine to medium sandstone matrix. Channel lag is overlain by parallel inclined laminated fine sandstone.

Figure 12. Geophysical log from Loyce Phillips #1 Yates (AA-38-12-322) illustrates the dominance of thin sandstones and fine-grained flood-plain deposits in interchannel facies.

Figure 13. Dip-oriented cross-section Y-Y' located in Figure 3. Cross section is positioned within interchannel facies and parallels cross section Z-Z' located 5 to 15 km (3 to 9 mi) to the east. Mudstone dominates the section. The greatest amount of sandstone occurs in the rim synclines flanking Palestine Salt Dome.

Figure 14. Contour map of the number of lignite beds in the undivided Wilcox (Kaiser, 1974) overlain on a facies map of the upper one-third of the Wilcox. Lignites are associated with interchannel areas around Oakwood, Palestine, and Boggy Creek Salt Domes. The contour of 100 ft net sandstone greater than 20-m outlines channel facies; arrows show the thickest accumulations of sandstone and the main axes of sediment transport. The down dip pinch out of dip-oriented sandstone greater than 20-m suggests that the depositional setting of the upper Wilcox included deltaic and possibly mud-rich coastal plain environments.

Figure 15. Dip-oriented cross-section X-X' located in Figure 3, modified from unpublished data by Kaiser, Johnston, and Bach (1978) figure 6, cross-section C-C'. Southward thickening of deltaic facies is illustrated. In southern part of study area a transgressive phase marked the termination of Wilcox deposition.

Figure 16. Three SP and resistivity logs around Oakwood Dome show facies interpretations and the nature of the ground water anomaly. The anomaly is thick and coincides with deltaic strata in KA-39-32-901 and KA-38-25-501 (located in fig. 21). Sandstones are characteristically thin and occur in upward-fining sequences. Deltaic facies are also thick in TOH-2A0 but only lower deltaic front facies below depth 2100 ft shows typical response of SP curve.

Figure 17. Three geophysical logs show relationship of ground-water anomaly and depositional facies around Oakwood Dome. Ground-water anomaly is characterized by negative deflection of SP curve. Only lower one-half of deltaic facies in TOH-2A0 has negative deflection of SP curve. This log response is typical for lower deltaic facies throughout the study area. Thick deltaic facies in KA-38-25-501 and KA-39-32-901 are characterized by negative deflection of SP curve. Main control on distribution of anomaly zone is uncertain. Anomaly may be affected by low permeability in deltaic strata, faults in Wilcox strata, or dome dissolution.

Figure 18. Histograms of relief and percentage surficial sand over 39 Texas coastal domes in the area near Houston to Beaumont-Port Arthur (fig. 1). Data is from the Fisher and others (1972, 1973) and McGowen and others (1976).

Figure 19. Map of the distribution of surficial sand and shallow salt domes in the Beaumont-Port Arthur area (modified from Fisher and others, 1973). Although the map area is subequally covered by sand and mud, only one dome, Spindletop, is overlain by approximately 50 percent surficial sand. The surface over the remaining six domes is covered by less than 25 percent surficial sand.

Figure 20. Map of dome uplifts and rim synclines. The largest rim syncline is associated with rapid growth of Bethel Dome during Wilcox deposition. The largest uplifted area over Boggy Creek Dome is probably related to large volume of salt in Boggy Creek salt structure. Absence of rim syncline or domal uplift indicates that Concord Dome was quiescent during Wilcox deposition. The fold axes of rim synclines are aligned in two trends. A western trend, oriented north-south, is associated with Bethel, Butler and Oakwood Domes. An eastern trend, oriented northeast-southwest, is associated with Boggy Creek, Brushy Creek, Keechi, Palestine, and Oakwood (?) Domes. This alignment may be related to growth from two parent salt ridges at depth.

Figure 21. Fence diagram of compressed cross sections across study area (located in fig. 3). The variation in sandstone greater than 20-m (black), sandstone less than 20-m (blank) and mudstone is shown in a strike and dip direction. Sandstone in the central one-third of the Wilcox is interconnected to a greater degree than sandstone in the upper one-third.

Figure 22. Strike-oriented cross section B-B' located in Figure 3. Cross section is oriented east-west across Bethel Dome and associated rim syncline. Fluvial channel-fill sandstones greater than 15 m (50 ft) thick are correlated. Rapid subsidence in rim syncline promoted development of stacked channel-fill facies. Only one channel-fill sand body occurs in uplifted area over dome.

Figure 23. Location map for wells, core and cross section V-V' around Oakwood Dome.

Figure 24. Isopach map, Wilcox Group. Rapid over-dome thinning occurs around Oakwood, Keechi, Brushy Creek, and Bethel Domes and probably around Butler Dome (insufficient data). No thinning occurs over deeply buried Concord Dome.

section over Oakwood Salt Dome (Fig. 17). The Wilcox is thinnest in this area over the dome and is in contact with the dome caprock. Note that the Wilcox over the dome is predominantly fine-grained mudstones and the sandstone that is present occurs in very thin beds less than 10 m (30 ft) thick.

Figure 26. Isopach map Wilcox Group in vicinity of Oakwood Dome (after unpublished data from A. Giles).

Figure 27. Generalized lithofacies cross section around Oakwood Dome based on maps of net sandstone greater than 20 m in Appendix 3. Sandstone distribution within each Wilcox layer is greatly simplified and is shown as a single value (compare to fig. 28). Area of thick net sandstone greater than 20 m occurs southwest of dome. Dome is surrounded by area of low net sandstone greater than 20 m. The low sand area around the dome is largest in lower (oldest) Wilcox layer (Appendix 3) and is smallest in upper (youngest) Wilcox layer.

Figure 28. Cross-section V-V' near Oakwood Dome located in Figure 18. A rim syncline southeast of the dome contains abundant stacked channel-fill sandstones. Immediately adjacent to (within 1 km; 0.6 mi) and over the dome, mud-rich interchannel facies are dominant. Extreme changes in percentage sandstone occurring in very short lateral distances (within 6 km; 4 mi) of Oakwood Dome are characteristic of similar facies changes around other domes in the study area.

#### TABLES

1. Depth, and boundary relationship of the domes are compared to Wilcox thickness and facies changes in the study area.

## ABSTRACT

Facies of the Wilcox Group preserve a record of syndepositional salt dome growth at the southern end of the East Texas Basin during the Eocene. Wilcox strata are thin and comprise mud-rich lithofacies immediately adjacent to and over the crests of domes that underwent relative domal uplift during Wilcox deposition. Concurrent with dome growth, migration of salt into the stock caused subsidence and overthickening of rim synclines and promoted development of sand-rich fluvial facies at greater distances from rising salt structures. Moderately buried (200 to 1000 m; 520 to 3300 ft) domes that were tectonically active during Wilcox deposition had similar effects on thickness and facies relationships of Wilcox strata not intruded by domes. Diapir growth produced topographically high areas that deflected fluvial channel systems away from the domes. This caused preferred development of mud-rich lithofacies above the dome. The migration of salt from below the rim syncline into the growing stock caused local subsidence to exceed regional norms and this favored vertical aggradation of sand-rich fluvial lithofacies.

It is believed that preferential development of mud-rich lithofacies around salt diapirs favorably enhances their hydrologic stability. Computer modeling is currently in progress to test this idea.

## INTRODUCTION

Shallow salt diapirs in the East Texas sedimentary basin are presently under consideration as repositories of high level nuclear waste (Kreitler, 1980; Kreitler and others, 1980; Kreitler and others, 1981). Central to such an assessment is an understanding of how fresh meteoric ground water may affect long term dome stability through dissolution. In the East Texas Basin, the zone of fresh meteoric ground water includes the Wilcox Group which encases or surrounds the upper 100 to 500 m (330 to 1640 ft) of most shallow diapirs.

The distribution of Wilcox depositional facies may exert a strong control on flow directions and velocities of ground water around salt domes. The Wilcox is extremely heterogenous as a result of lateral and vertical variations in the distribution of highly permeable sands and other sandstones, mudstones, and lignites with low permeabilities. Variables affecting aquifer characteristics include thickness and hydraulic conductivity. These vary in part as a function of depositional facies and sand-body geometry including sandbody thickness, permeability, and interconnectedness.

This report provides the basic facies and sand body data for computer modeling ground water flow around Oakwood Dome (Fogg, 1980a). Two problems are addressed in this study (1) what is the facies distribution and sand-body geometry of sandstones with high hydraulic conductivities and the greatest potential for possible dome dissolution and (2) how is facies distribution affected by syndepositional dome growth.

The presence of actively growing shallow salt diapirs during Wilcox deposition is evidenced by variations in Wilcox lithofacies over domes and by rim synclines around domes. The presence of topographically high areas over salt structures and greater local subsidence in associated rim synclines

are inferred to have caused a characteristic near-dome facies assemblage. This assemblage includes mud-rich, low permeability interchannel facies over and immediately adjacent to growing diapirs and sand-rich, high permeability channel facies in rim synclines.

The study area covers approximately 1500 km<sup>2</sup> (900 mi<sup>2</sup>) in the southern part of the East Texas Basin. The area contains five shallow salt domes (less than 500 m; 1640 ft), two intermediate depth (greater than 500 m; 1640 ft, less than 1500 m; 5000 ft) domes, one deep (greater than 1500 m; 5000 ft) dome, deep salt structures, complex graben systems, and possible growth faults (fig. 1). The Wilcox Group is the first Tertiary fluvial-deltaic system to prograde entirely across the East Texas Basin and construct major "Mississippi-type" deltas at the northwestern margin of the Gulf of Mexico. Along the southern margin of the East Texas Basin, the Wilcox is composed primarily of an aggrading, highly meandering fluvial system (Fisher and McGowen, 1967) that constructed a major delta lobe--the Trinity lobe--80-250 km (50-150 mi) downdip (south) of the study area (fig. 2).

#### METHODOLOGY

This study is based on subsurface data. Maps (isopach, net and percentage sandstone, facies and structure contour) and cross sections (lithostratigraphic and compressed) (fig. 3) were prepared from over 300 self potential (SP) and induction resistivity logs (Appendix 1). One complete core through the Wilcox (LETCO TOH-2A0) 0.6 km (2000 ft) southeast of Oakwood salt dome provided hydrologic, lithologic, and geophysical data to improve correlations with other wells that only provided indirect (resistivity, self potential) data (fig. 3). Detailed lithologic descriptions of the core and associated geophysical logs are presented in Appendix 2.

Lithofacies data gathered in this study were input into a computer model of ground water movement and flux (Fogg, 1980b). Techniques employed in construction of maps and cross sections were intended to highlight hydraulic conductivity and aquifer interconnectedness, which along with topography and structure, are inferred to be the major controls on ground water movement and flux.

One key is this study as identifying sandstone with high hydraulic conductivity (permeability) that have the ability to rapidly transmit large volumes of water. Net and percentage maps of sandstone greater than 20 ohm-m<sup>2</sup>/m ( $\Omega$ -m) illustrate the distribution of highly resistive, highly transmissive sandstones. Hydraulic conductivities were related to resistivity measured on resistivity logs (Fogg, 1980b) through a series of pump tests, core permeability tests, and published values (fig. 4). Sandstones with resistivities greater than 20 ohm-m<sup>2</sup>/m ( $\Omega$ -m) have hydraulic conductivities from 1 to 3 orders of magnitude greater than sandstones with resistivities less than 20  $\Omega$ -m (Fogg and Seni, 1981; in preparation). The highly resistive sandstones are capable of transmitting 10 to 30 times more water than sandstones with lower resistivity. For modeling purposes ground water flux through less resistive sandstones can effectively be ignored.

In order to document vertical as well as lateral changes in lithostratigraphy, the Wilcox was divided into three layers of equal thickness. This slice technique (Jones, 1977) emphasized the depositional grain of sandstones by mapping a time-stratigraphic unit deposited in a shorter time interval than if the undivided Wilcox were mapped. Changes in sand body location and thickness are readily visualized by comparison of individual maps. A complete suite of maps of net and percent sandstone greater than 20  $\Omega$ -m was prepared for each layer and is presented in Appendix 3. These map layers cut across genetic facies sequences, but they are roughly equivalent to the

three-fold stratigraphic subdivision of the Wilcox (in ascending order the Hooper, Simsboro, and Calvert Bluff Formations).

Fourteen cross sections lines were laid in a grid across study area (fig. 3). Conventional cross sections were constructed and sandstone sequences and facies were correlated. For computer modeling, resistivity log data were reduced to three conditions--sandstone greater than 20  $\Omega$ -m, sandstone less than 20  $\Omega$ -m, and shale (mudstone)(Fogg, 1980b). The distribution and thickness of each of the three conditions was displayed on strip logs (Appendix 4). Compressed sections constructed from strip logs involved compression of space between logs along a line of section until the strip logs were side by side. This technique compressed distances between some wells unequally but correlations were readily visualized. In Appendix 4, six compressed cross sections are presented. The horizontal datum is the top of the Midway Group.

#### Limitations of study

Lithofacies mapping (Appendix 3 and 4) employed a narrow definition of sandstone, that is sandstone with resistivity greater than 20  $\Omega$ -m. This technique identified sandstones with the greatest impact on ground water flow, but caution must be exercised in use of this data for interpretation of depositional environments. In the study area mapping of highly resistive sandstones is biased toward recognition of thick fluvial channel sands because of 1) bed thickness affects and 2) relationship between ground water and depositional facies.

Resistivity curves measure the resistivity of pore fluids and host rock but are also affected by bed thicknesses and hole-diameter effects. According to Keys and MacCary (1971) resolution of induction resistivity curves is adversely affected when the bed being logged is less than 1.8 m (6.0 ft) and is several times more resistive than adjacent beds. The measured resistivity of thin beds is less than true resistivity. Thus, sandstone beds thicker than 1.8 m (6.0 ft) are preferentially recognized with a criteria of high resistivity.

Throughout the East Texas Basin, the base of fresh water commonly occurs in the Wilcox Group at the boundary between the fluvial and deltaic facies. Wilcox environments record a facies tract with fluvial facies updip and deltaic facies downdip. The accord with Walther's Law, progradation has deposited coarse-grained fluvial facies over fine-grained deltaic facies. Dip-oriented fluvial sands in the subsurface probably retain a connection with similar sandy facies exposed updip in the outcrop belt (Henry and Basciano, 1979, figs. 6 and 8). This connection allows fresh meteoric water to recharge permeable channel sands. The contrast, ground water velocities are probably much slower in deltaic sands that are isolated to a greater degree and interbedded with marine clays. In the study area, few deltaic sands have resistivities greater than 20  $\Omega$ -m except near the outcrop belt.

A downdip change in water quality (decreased resistivity, increased total dissolved solids, salinity, or chlorinity) is commonly observed in regional ground water studies (Back, 1960; Toth, 1972; Galloway, 1977; Galloway and Kaiser, 1980). This change is related to a general increase in residence time for ground water in the subsurface. Sandstones containing ground water with high resistivities, then are assumed to outline areas recharge and active ground water flux (Galloway and Kaiser, 1980). These areas generally coincide with dip-oriented fluvial axes.

Upward leakage of deeper saline ground waters along faults is probably occurring along the Mount Enterprise-Elkhart Graben in southern Anderson and Cherokee and northern Houston Counties (Fogg, 1980d). This may affect the distribution of sandstones greater than 20  $\Omega$ -m in the vicinity of the faults.

#### Terminology

To facilitate greater understanding a few terms will be defined. Rim syncline is a structural depression that flanks and partially or completely surrounds domes (Kupfer, 1970). The rim syncline is used synonymously with the localized isopachous thick associated with the filling of the depression from lateral flow of salt into the diapir.

The pre-Wilcox growth history will not be described for diapirs in the area. The lack of post-Wilcox deformation indicates that the form and depth of diapirs today is basically similar to their form and depth during deposition of the Wilcox. Domes with large rim synclines in Wilcox strata had greater relative vertical movement than did domes with rim synclines that were small are absent. Domes in contact with the Wilcox are inferred to have intruded the Wilcox. No domes in the study area have penetrated completely through the Wilcox or are in contact with younger strata. Controversy surrounds the interpretation of diapiric growth and hinges on whether intrusion (Nettleton, 1934; Trusheim, 1968; Kupfer, 1970) or extrusion (Loocke, 1978; Bishop, 1978) is the dominant process.

## DEPOSITIONAL SYSTEMS

An understanding of depositional systems and sand-body geometry is critical to studies of how ground water flows around domes. In the study area salt domes occur within areas dominated by fluvial deposits and syndepositional dome growth has controlled the distribution of channel facies. The fluvial system is divided into channel and interchannel facies on the basis of net sandstone and sand-body geometry. Six of the eight salt domes occur entirely within fine-grained interchannel facies or at the boundary between channel and interchannel facies.

## Regional Stratigraphic Framework

Cyclic sedimentation during the Eocene (Fisher, 1964) has resulted in deposition of alternating marine and fluvial-deltaic sequences (fig. 5). This regional framework is an important factor affecting movement of ground water. Marine Midway shales underlie the Wilcox and act as a regional aquitard dividing the predominantly meteoric ground water section in the Wilcox from a lower saline section (Fogg, 1980c). This regional pattern of ground water flow is more complex around salt domes and in areas of regional faults (Elkhart Graben-Mt. Enterprise Fault System) (Fogg, 1980c). The Carrizo Sandstone (Claiborne Group) overlies the Wilcox and is a widespread fluvial sheet sandstone that is a major regional aquifer interconnected with the Wilcox aquifer.

In many areas, the Wilcox Group is divided into three formations, in ascending order, the Hooper, the Simsboro, and the Calvert Bluff. The Wilcox is undivided in the eastern half of the study area because the Simsboro is no longer present as a continuous, thick sandstone between the dominantly clay-rich Hooper and the sandy and clayey lignite-bearing Calvert Bluff. The traditional formal nomenclature is not used in this study in favor of genetically based concepts of depositional systems.

The regional depositional systems framework was first described by Echols and Malkin (1948). Fisher and McGowen (1967) described Wilcox depositional systems including the Mt. Pleasant fluvial system over the East Texas Basin, the Pendleton bay-lagoon system further east, and the Rockdale delta system (Echols and Malkin, 1948) south of the East Texas Basin (fig. 2). Strand plain, bay-lagoon, barrier bar, and shelf systems occur further south and west of the study area and are not considered in this study. Kaiser (1974) and Kaiser, Johnston, and Bach (1978) mapped

Wilcox sand-body geometry and the occurrence of lignite. They largely confirmed Fisher's and McGowen's interpretations with regard to the Mt. Pleasant fluvial system. Kaiser, Johnston, and Bach (1978) also described a thin deltaic section at the base of the Wilcox between the marine Midway shales and the Mt. Pleasant fluvial system.

Two depositional systems -- fluvial and deltaic--occur in the study area and are described below.

## Fluvial System

Fluvial system deposits overlies deltaic strata in the study area where the Wilcox is composed of fluvial strata ranging in thickness from 150 to 500 m (fig. 2). Two fluvial facies--channel and interchannel--were identified. The distribution of these facies, their sand-body geometry, and thickness patterns strongly suggest that these facies have different effects on the hydrologic stability of salt domes.

Channel sandstones that are thick, permeable, and interconnected may adversely affect dome stability because of the potential for circulating ground water to cause dome dissolution. A dome that pierces sand-rich channel facies has a greater probability of being affected by dissolution than a dome that pierces sand-poor interchannel facies because of the difference in aquifer properties of the two facies.

Salt domes in the study area are preferentially located in mud-rich interchannel facies because localized uplift from dome growth formed areas of slightly more positive relief over the dome and caused fluvial channels to flow around the uplifted areas.

### Channel facies

Dip-oriented axes of thick net sandstone and high percentage sandstone outline fluvial channel facies in Figure 6. In the lower one-third of the Wilcox, fluvial facies grade to the south into deltaic facies (fig. 7) where dip-oriented sandstone trends become lobate.

Three to five major alluvial sandbelts traverse the study area from north to south (figs. 6 and 7; Appendix 3). The thickest belts occur in central Anderson County. The eastern part of the study area is sand-rich with sandstone belts coalescing and trending east-south-east. The western part of the study area is mud-rich.

Channel facies are composed primarily of channel-fill sandstones that are dip-oriented and vertically stacked. Dip-oriented belts with greater than 100 ft net sandstone greater than 20  $\Omega$ -m define channel axes for the three Wilcox layers (Appendix 3). Channel-fill sandstones are a minor component of interchannel facies where they occur relatively isolated in fine-grained overbank sediments. Channel facies sandstones tend to be more resistive on induction resistivity logs because they are fresh-water aquifers that are presumably connected to other fluvial sandstones exposed updip in the outcrop belt. The channel axes in Figure 6 agree well with the orientation of fluvial sandstone patterns mapped regionally by Fisher and McGowen (1967) and Kaiser, Johnston, and Bach (1978). Figure 6 includes the central one-third of the Wilcox Group and represents portions of both the Simsboro and Calvert Bluff Formations.

Packages of thick channel-fill sandstone are recognized on self-potential and induction resistivity logs by their thick blocky pattern (fig. 8). Major channel-fill sandstones are stacked vertically in packages 50 to 300 m (160 to 1,000 ft) thick and occur in belts 6 to 30 km (4 to 18 mi) wide. Individual channel sand bodies are much thinner (8 to 60 m; 26 to 200 ft) and narrower (0.4 to 3.2 km; 0.2 to 2 mi). A dip-oriented cross section (fig. 9) down the central fluvial axes in Anderson County illustrates the connectedness and vertical stacking of major sand bodies. Figure 10 is a strike-oriented cross section that displays the relationship between channel facies and sand-poor interchannel facies. Comparison of these two cross sections shows interconnectedness is much greater in a dip direction.

A core of a small channel-fill sand body (LETCO TOH-2A0) is characterized by an upward fining textural trend (Appendix 2) and stratification similar to deposits of Mississippi River-type suspended load streams

Fisher and McGowen, 1967; Kaiser, 1974). Although the core is in inter-channel facies, the stratification and textural trends are similar to channel-fill deposits in the channel facies. The channel-fill is floored by a channel lag composed of intrabasinal mud clast conglomerate (fig. 11). The matrix is a fine to medium sandstone. The mud clasts are imbricated with a maximum long dimension of 5 cm. Parallel-inclined silty, very fine to fine sandstone (fig. 11) overlies the channel lag. Parallel-laminated and rare trough-fill cross stratified, very fine to fine sandstone comprise the bulk of the channel-fill. Thin clayey, very fine to fine sandstone laminae (0.5 to 2.0 cm) are interbedded with cleaner sandstone in the upper part of the channel-fill sequence. Overbank and levee deposits overlie the channel-fill. Parallel-laminated and rippled clayey siltstone and very fine sandstone are interbedded with parallel-laminated silty clay that contains abundant macerated plant debris.

The upward fining textural trend, relatively high mud content, and sequence of primary sedimentary structures indicate the fluvial system was similar to Mississippi River-type suspended load streams. The Brazos River (Bernard and others, 1970) is another modern analogue of Wilcox fluvial systems that may be more applicable due to similarities in the size of deposits. According to Bernard and Majors (1963), the typical thickness of Brazos River fluvial meanderbelt deposits is 17 m (55 ft) and the width of the meanderbelt is 2.5 km (1.5 mi).

#### Interchannel facies

Interchannel facies preferentially encase the upper 100 to 500 m of shallow salt diapirs in the study area (figs. 6 and 7; Appendix 3).

The transition from channel to interchannel facies is characterized by a decline of 30 to 60 percent in percentage sandstone greater than 20  $\Omega$ -m.

Interchannel facies flank channel axes (figs. 6 and 7) and occur as belts 5 to 35 km (3 to 21 mi) wide. In Figures 6 and 7, the interchannel facies includes the area with less than 100 ft sandstone greater than 20  $\Omega$ -m. Interchannel facies contain 0 to 20 percent sandstone greater than 20  $\Omega$ -m. In contrast, channel facies contain greater than 40 percent sandstone greater than 20  $\Omega$ -m. The sandstone present in interchannel facies is predominantly thin, silty and clayey sandstones. Clean, resistant, channel-fill sandstones are rare.

Log characteristics of interchannel facies illustrate the abundance of thin sandstones that commonly are 0.5 to 4.0 m (1.5 to 13 ft) thick and range in thickness up to 30 m (100 ft) (fig. 12). The sandstones are interbedded with thin (0.5 to 10 m) to thick (greater than 20 m) mudstones and commonly lignite. Crevasse channel, crevasse splay, thin tributary channel-fill, lacustrine delta, and levee deposits are the relatively sandy components of interchannel facies. They tend to be poorly interconnected and are relatively isolated in fine-grained floodbasin deposits.

A strike-oriented cross section (fig. 10) through interchannel and channel facies contrasts the difference in sandstone percentage, sand body thickness, and connectedness. In a dip-direction (fig. 13), interchannel sandstones are better connected than in a strike section, but they remain isolated with a fine-grained matrix.

Lignite is an important component of Wilcox interchannel facies (Kaiser, 1974; Kaiser and others, 1978). Lignites were not differentiated in this study because, like mudstones, lignites are relatively impermeable and would have similar effects on the flow of ground water. According to Kaiser (1974), fluvial lignite occurs between paleochannels where

backswamp peats formed in interchannel areas. Deltaic lignite also occurs as a component facies in the Rockdale delta system (Fisher and McGowen, 1967). Kaiser (1974) mapped the number of individual lignite beds. A contour map of these data (fig. 14) shows the greatest number of lignite occurrences are closely associated with the fine-grained interchannel deposits around Oakwood, Palestine, and Boggy Creek salt domes and in interchannel areas along the present day Trinity River, south of the Leon-Freestone County line, and in the western part of the map area. Environmental conditions associated with dome growth during Wilcox time were evidently favorable for accumulation of lignite and must have been basically similar to normal floodbasin conditions.

Descriptions of core from near Oakwood Dome (Appendix 2) show that interchannel facies were characterized by finely interlaminated, silty, very fine sandstone and mudstone. Organic matter was abundantly preserved; it occurs as thin lignite beds (0.01 to 0.6 m) and as macerated plant debris in both mudstones and sandstones. Sedimentary structures also are largely preserved and include parallel laminae and ripples with rare scour surfaces. Thin, channel-fill deposits also occur in the core. The channel-fill is upward-fining and ranges in thickness from 1 to 30 m. Unlike coarse-grained deposits in the channel facies, channel-fill in the interchannel facies is not vertically stacked.

#### Delta System

At the base of the Wilcox a thin, progradational delta system conformably overlies marine and prodelta shales of the Midway. South toward the Gulf of Mexico the delta system expands up to 1500 m (5000 ft) to form the Rockdale delta system. In the study area the delta sequence is from 40 to 300 m (130 to 1000 ft) thick and thickens toward the south

and southeast. Thin transgressive deltaic deposits are probably interbedded with the uppermost fluvial section equivalent to the Calvert Bluff (Kaiser, Johnston, and Bach, 1978) over much of the study area. The thin progradational nature of the lowermost Wilcox deltaic section within the East Texas Basin contrasts with the massive thickness (up to 1500 m; 5000 ft) and aggradational character of Wilcox deltaics further downdip toward the Gulf of Mexico.

The significance of deltaic deposits to questions of hydrological stability of salt domes is related to: (1) deltaic facies around salt domes and (2) to the occurrence of anomalous ground water in deltaic facies around Oakwood Dome.

#### Deltaic facies

The relationships between deltaic facies and dome growth in Wilcox time are not as clear as with fluvial deposits. The transitional nature of fluvial and upper delta plain environments makes it difficult to define an exact boundary between fluvial and deltaic systems. Despite the difficulty in separation of transitional fluvial-deltaic environments, the distribution of deltaic facies are characterized by the occurrence of thick deposits around Oakwood Dome and in the southern part of the study area.

Deltaic system deposits are largely confined to the southern one-third of the study area (fig. 7) where they approach one-half of the total thickness of Wilcox deposits (fig. 15). The thickest deltaic deposits occur in the vicinity of Oakwood Dome. In the southern part of the study area the sand-body geometry varies from lobate to strike-oriented and contrasts with the strong dip-oriented trend in the fluvial section. Strike-oriented sandstone trends are influenced by growth faulting

along the Mt. Enterprise-Elkhart Graben system. A net sandstone map of the lower one-third of the Wilcox shows the lobate pattern well-developed in Leon County (fig. 7; Appendix 3). Dip-oriented fluvial trends coalesce and form broad areas of thick net sand with consistent percentage sand. In earliest Wilcox time, a small delta prograded across the East Texas Basin to form a lobate deposit in northern Leon and Houston Counties. This thin delta sequence was deposited on a relatively stable platform and predates the massive aggradational deltaic deposits further downdip. The Guadalupe delta (Donaldson and others, 1970) is a possible modern analogue.

Although at least three deltaic facies can be distinguished by distinctive log patterns, deltaic facies were grouped into a single class of deposits. Characteristic log patterns are shown on resistivity and self-potential logs from Law Engineering Testing Company TOH-2A (fig. 16). Both upper Midway and basal Wilcox strata display an upward-coarsening log pattern characteristic of delta front deposits. Individual frontal splays also coarsen upward and range in thickness from 3 to 12 m (10 to 40 ft). The Midway-Wilcox contact is arbitrarily defined as the lowest locally mappable upward-coarsening sand body. These thin frontal splays are mappable over broad areas (100 to 500 km<sup>2</sup>; 36 to 180 mi<sup>2</sup>) and represent the best available time markers.

Delta front deposits are overlain by delta plain or delta platform strata that consist of interbedded sandstone and mudstone. Delta plain facies generally occur below massive fluvial sandstones. The log pattern of delta plain deposits is very similar to the log pattern of interchannel facies, but differences in bounding relationships with component facies serve to distinguish between the two facies.

The occurrence of glauconite and organic matter provided evidence on the deltaic origin of lowermost Wilcox strata. Organic matter is

especially abundant in fluvial and delta plain environments and occurs as both individual beds and as macerated plant debris (Appendix 2). Organic matter becomes rare and occurs only as macerated plant debris in the delta front environment where it was transported along with the sand- and silt-sized fraction.

The distribution of glauconite shows an inverse relationship with organic matter. Glauconite occurs in greatest abundance (~20%) in lower-most delta front sandstones. Occasional glauconite pellets occur in delta plain strata and were possibly deposited during minor delta desiccation phases. Glauconite is rare to absent in the fluvial section. Periods of deltaic sedimentation were interrupted by local marine transgressions during delta foundering.

#### Ground-water anomalies in deltaic facies

Fogg (1980c) described a saline anomaly in Wilcox sandstones in ten wells around Oakwood Dome. Fogg noted that the anomaly occurred in a zone near the base of the Wilcox characterized by muddy sandstones and that the anomaly was absent in clean sandstones in the upper parts of the Wilcox. The anomaly is apparently restricted to a range of deltaic sand bodies. Growth faulting may be a factor affecting the location of the anomaly.

A comparison of two logs from inside and one log just outside the anomalous zone (fig. 17) shows that the anomaly is apparently restricted to deltaic facies. The anomaly occurs in the middle and lower sections of the Wilcox and is characterized by a negative deflection in the self-potential (SP) curve of 20 to 60 millivolts (mv).

Sandstones in the anomalous zone are characteristically thin (0.5 to 10 m; 2 to 33 ft; maximum 15 m; 50 ft) and are interbedded with mudstones

with subequal thicknesses. Stacked channel-fill sandstones are absent in the anomalous zone.

Thin, delta front sandstones in the widespread deltaic section at the base of the Wilcox are also characterized by a negative SP deflection of from 20 to 40 mv. These lowermost delta front sandstones are interbedded with and encased within marine Midway shales. The interstitial fluid is typically "saline" as characterized by the negative SP deflection throughout the study area. Fluids in this zone are not considered anomalous.

With present data it is not possible to state unequivocally if the ground-water anomaly is a saline anomaly characterized by a preponderance of  $\text{Na}^+$  and  $\text{Cl}^-$  ions and due to present or past dome dissolution. The association of the anomaly with deltaic facies and the absence from thick channel-fill facies is interpreted to indicate the anomaly is unrelated to modern dome dissolution. Fogg (1980c) noted that the anomaly may represent dissolution of Oakwood Dome at some time in the geologic past, presumably during deposition of the Wilcox. Alternately the anomaly may represent connate (dominantly marine) interstitial fluids that were trapped in low permeability deltaic sandstones surrounded by and interbedded with marine clays. This interpretation is supported, in part, by Fogg (1980a), who showed a regional correlation between mud-rich zones in the Wilcox and the presence of brackish waters. Possible sources of saline waters were related to marine inundations, to very slow ground-water velocities (0.15 to 61 m/million years; 0.5 to 200 ft/million years), or to dome dissolution in the geologic past.

#### Modern Analogue

A modern analogue for Wilcox deposits includes the Mississippi River and delta system (Kaiser, 1974; Kaiser, Johnston, and Bach, 1978; Fisher

and McGowen, 1968; Galloway, 1968). The Simsboro Sand is central sand-rich zone of the Wilcox that fits the Mississippi River model and the very thick deltaic section south of the study area fits the Mississippi delta model. However, Wilcox deposits in the study area do not fit the Mississippi model of either environment very well because in this area deltaic deposits are very thin and the widespread Simsboro Sand pinches out.

One possible Modern analogue for Wilcox depositional setting in the study area is the Modern upper Texas coastal plain from Bay City-Freeport area southwest of Houston to Beaumont-Port Arthur. This flat, marshy terrain is traversed by eight major drainages (San Bernard, Colorado, Navidad, Brazos, San Jacinto, Trinity, Neches, and Sabine Rivers) and contains abundant shallow salt diapirs. Active Holocene oceanic deltas on the upper Texas coast include the Brazos and Colorado deltas. Bayhead or estuarine deltas include the Trinity and San Jacinto deltas in Galveston and Trinity Bays, respectively. Because of the low sediment load, the Neches and Sabine Rivers are not forming deltas at their confluence with Sabine Lake. Regional subsidence is the dominant influence in the area, but because the major Holocene depocenter--the Mississippi delta--is 250 to 400 km (150 to 250 mi) to the east, the rates of sedimentation and subsidence have slowed during the Plio-Pleistocene. This setting is somewhat analogous to the shift of major Wilcox deltas 80 to 250 km (50 to 150 mi) downdip from the study area. Relief on the Texas coastal plain is very low and the slope ranges from 0.04 to 0.10 m/km (0.2 to 0.5 ft/mi).

The presence of shallow salt diapirs is an important aspect of the depositional model. Along the Texas Coastal Zone surface mapping (Fisher and others, 1972, 1973; McGowen and others, 1976) has provided valuable information on topographic relationships and surface sand distributions over domes.

Most shallow diapirs (56 percent have greater than 5 ft relief) along the Texas coast have positive surface expression (fig. 18). Surface relief over the domes ranges from negligible to over 20 m (66 ft) at Damon Mound. The lack of relief over some salt structures is probably related to their greater depth of burial.

Texas coastal zone diapirs display a weak preference (85 percent significance level  $\chi^2$  test for 39 shallow domes) to occur in areas lacking surficial sand deposits (fig. 18). The locations of shallow domes in the coastal zone and the distribution of surficial fluvial sand and clay deposits are shown near Beaumont-Port Arthur (fig. 19). In this area diapirs are clearly associated with areas of mud-rich surficial deposits. Facies and environments tend to stack vertically by aggradation in regions that are subsiding rapidly. Kreitler and others (1977) have shown that sandstones are vertically stacked in upper Pliocene and Pleistocene fluvial-deltaics in the Houston-Galveston area. The location of coastal diapirs in mud-rich surficial deposits indicates a high probability that the diapirs are encased by older deposits that are also mud-rich.

## LITHOFACIES FRAMEWORK AND SALT TECTONIC ACTIVITY

Salt tectonic activity has affected the distribution of Wilcox depositional facies, the occurrence of lignite resources, structure and fault systems. Analysis of the Early Cretaceous to Tertiary depositional history of the East Texas Basin (Kreitler and others, 1981) and facies associated with shallow salt domes in the study area indicates the following:

1) Prior to Wilcox time, the shallow diapirs in the study area had already formed.

2) Thickness and facies changes both over and on dome flanks indicate that dome growth continued during Wilcox sedimentation.

3) The Wilcox is thin and is characteristically composed of fine-grained interchannel facies over and adjacent to (within 1 to 3 km; 0.6 to 2 mi) salt domes. These lithofacies were deposited, as uplift from dome growth maintained a positive topographic anomaly during regional subsidence. This topographic high deflected fluvial channel systems from the immediate area of the dome. There was still net accumulation of sediment over the crest of the dome due to the greater influence of regional subsidence.

4) The Wilcox is thick and characteristically composed of coarse-grained channel-fill facies in rim synclines flanking the domes (within 5 to 15 km (3 to 10 mi) because subsidence due to salt withdrawal is added to regional subsidence.

5) The absence of facies changes of rim synclines indicates relative dome stability during Wilcox time.

6) The East Texas coastal plain (McGowen and others, 1976; Fisher and others, 1972, 1973) between Houston and the Louisiana border is a possible Modern analogue with similar dome growth patterns and effects.

Opposing processes--uplift and subsidence--operated simultaneously and in close spatial context during dome growth. These two processes had opposite effects on Wilcox lithostratigraphy over short (1 to 15 km; 0.6 to 10 mi) lateral distances. Domal uplift and diapiric intrusion through Wilcox sediments caused thinning and development of sand-poor lithofacies immediately adjacent to and over the dome crest. Concurrently, subsidence in rim synclines caused thickening of Wilcox strata and preferred development of sand-rich lithofacies at greater distances from the dome (fig. 20).

A summary of the regional lithofacies variations of the Wilcox in the study area is shown in Figure 21. The Wilcox is clearly heterogeneous in both a lateral and vertical sense. The lower one-third is mud-rich and is deficient in sandstone greater than 20  $\Omega$ -m. Continuity of the mudstones and sandstone in the lower section is high. The central one-third contains the greatest amount of sandstone greater than 20  $\Omega$ -m. Lateral continuity is variable and ranges from high in cross section F-F' to low in cross sections E-E' and I-I'. The upper one-third contains less sandstone greater than 20  $\Omega$ -m and is the most heterogeneous section. The lateral persistence of the overlying Carrizo Formation is especially evident in cross sections B-B' and K-K'.

Table 1 summarizes data on dome movement in Wilcox time and present depth to diapir. Evidence suggests that diapiric activity during Wilcox time is not solely a function of depth of burial of individual diapirs. Even domes at moderate depths that are not in direct contact with Wilcox strata may strongly influence thickness and depositional facies.

Sandy-body geometry and location are affected more strongly by shallow domes (less than 500 m; 1640 ft subsurface) than by deep domes. All five

shallow domes are in fine-grained interchannel facies, but the two intermediate depth domes (Brushy Creek and Boggy Creek Domes) had only limited effect on sand-body distribution.

The percentage overthickening of sediments in rim synclines (comparison of thickness of rim syncline to local norms) is the best indicator of relative amounts of upward dome growth. The volume of salt migrating into the stock is equal to the volume of overthickened sediment in the rim syncline. The trends of overthickening in rim synclines around the shallow domes were erratic and ranged from 8 to 47 percent thicker than local norms. Rim synclines around the intermediate depth domes were 23 and 33 percent overthickened around Brushy Creek and Boggy Creek, respectively. The two intermediate depth domes showed greater upward growth and volumes of salt movement than three of the five shallow domes.

Facies distribution around Bethel Dome (fig. 22) illustrates the effect of salt mobilization associated with a moderately buried (430 m; 1411 ft subsurface) salt dome. The rim syncline (fig. 20) east of Bethel Dome is the site of stacked channel-fill facies where up to five fluvial sand bodies are over 15 m (50 ft) thick. In contrast, only one sand body over 15 m (50 ft) thick occurs in the uplifted area over Bethel Dome.

#### Oakwood Dome

The effects of lithofacies variations on ground-water flow around Oakwood Dome are currently being computer modeled (Fogg, 1980b; Fogg and Seni, 1981; Fogg and Seni, in preparation). The area around Oakwood Dome (fig. 23) illustrates typical facies response to syndepositional growth of shallow salt diapirs (fig. 24). Up to 300 m (1000 ft) of thinning occurs over Oakwood Dome (Giles, 1980) (fig. 25). The thinned strata (fig. 26) extends less than 2 km (1.2 mi) from the approximate outline of the salt

stock. A small fault is associated with a rim syncline southwest of the dome that extends to the northeast. The rim syncline is 8 percent thicker than local areas unaffected by salt diapirism. The size and thickness of the rim syncline around Oakwood Dome is typical of other synclines in the study area (Table 1).

In Appendix 3, maps of sand-body geometry (particularly net sandstone greater than 20  $\Omega$ -m) clearly illustrate the minor amount of sandstone greater than 20  $\Omega$ -m over and around Oakwood Dome. Lithofacies data from Appendix 3 are generalized in Figure 27 to show the vertical distribution of sandstone greater than 20  $\Omega$ -m in the area around Oakwood Dome. A low net sand area of less than 50 ft sandstone greater than 20  $\Omega$ -m (for each layer of the Wilcox) overlies and extends 2 to 8 km (1.2 to 4.8 mi) around Oakwood Dome. The area of low net sand surrounding the dome becomes smaller with each successive map layer.

Dip-oriented thick net sand belts occupy rim synclines around Oakwood Dome. More than 200 ft of sandstone greater than 20  $\Omega$ -m occur in rim synclines 8 to 14 km (4.8 to 8.6 mi) southwest and 2 to 8 km (1.2 to 4.8 mi) northeast of the dome.

A cross section near Oakwood Dome illustrates both thickness and local facies changes (fig. 28). Channel facies comprising multiple stacked channel-fill sandstones occur in the rim syncline 3 to 10 km (2 to 6 mi) southeast of Oakwood Dome. Interchannel facies dominate over the dome where only thin packages of sandstones are interbedded with mudstones. Note that, not only does percentage sandstone decrease (Appendix 3), but that individual sand bodies become much thinner and undoubtedly less continuous. It is rare that well control is dense enough to map this facies transition.

The localized effect of salt diapirism is often not readily detectable because (1) thickness and facies changes occur over a lateral distance that may be less than available well spacing, (2) facies changes from dome growth resemble similar facies changes in areas unaffected by dome growth, and (3) well spacing and/or thickness of contour interval may not be fine enough to detect thickness changes.

#### RECOMMENDATIONS

This study represents a step toward detailed understanding of ground-water flow in Wilcox strata around salt domes, specifically Oakwood Dome. In addition to a better understanding of localized Wilcox facies and ground-water flow, this study develops techniques that have wide applicability to dome stability problems in other salt basins.

The techniques include identification and mapping of facies characteristics (especially hydraulic conductivity, thickness, and sand-body geometry) with the greatest potential impact on hydrologic stability of

domes. Detailed facies mapping in the vicinity of salt domes has highlighted the variability of sediments and facies as a result of syn-depositional dome growth. This variability and the requirement to understand this variability for modeling purposes underscores the need for very dense subsurface control with a spacing less than the average distance over which facies changes occur.

The methodology employed in this study is directly applicable to other Gulf Interior Salt Dome Basins in Louisiana and Mississippi. Rayburn's Dome in Louisiana and Richton Dome in Mississippi both intrude Wilcox strata. The location of sand-rich facies in rim synclines with respect to dome flanks would have an important bearing on dome stability because the two domes have intruded through mud-rich facies originally deposited over the domes. Miocene terrigenous clastics over Richton Dome also could be studied with techniques similar to those used in this study.

#### SUMMARY AND CONCLUSIONS

During periods of regional subsidence, growth of shallow salt diapirs produces diagnostic facies relationships in the sedimentary record. Such a record is preserved in the Eocene Wilcox Group at the southern end of the East Texas Basin.

The Wilcox is characteristically thin (10 to 80 percent thinning) in a 10 to 30 km<sup>2</sup> (4 to 9 mi<sup>2</sup>) area immediately over the salt stock. The Wilcox is characteristically thick in rim synclines (5 to 50 percent overthickened) over a 20 to 75 km<sup>2</sup> (7 to 25 mi<sup>2</sup>) area on dome flanks or in a torus surrounding the dome. Thickness and structural changes are usually more subtle for domes that are deeply buried.

Dome growth produced topographic highs and influenced facies changes both over the dome and on dome flanks. Over dome areas are characteristically mud-rich interchannel areas. During complete intrusion or extrusion of the diapir this facies record is lost.

Stacked channel-fill facies occupy rim synclines because subsidence greater than regional norms favors aggradation and vertical stacking of depositional environments. Rim synclines have a higher preservation potential during burial and continued domal intrusion. Even with complete intrusion or if complete salt loss is postulated, the sedimentary record is preserved in the rim syncline.

At the present time any effect on hydrological stability of domes by lithofacies variation is conjectural. Even with dense regional well control on the order of one well every  $9 \text{ km}^2$  ( $3 \text{ mi}^2$ ), some local features will be missed. Factors tending to enhance dome hydrologic stability include development of less permeable mud-rich lithofacies over and immediately adjacent to domes. But, sand-rich channel facies occupying rim synclines on dome flanks may adversely impact dome stability through dissolution. The delineation and understanding of three-dimensional sand-body geometry is a step toward a more accurate prediction of the interaction of ground water and salt diapirs and of the importance of rapid facies variability as a result of syndepositional dome growth.

- Anderson, R. E., Eargle, D. H., and Davis, B. O., 1973, Geologic and hydrologic summary of salt domes in Gulf Coast Region of Texas, Louisiana, Mississippi and Alabama: U.S. Geol. Survey Open-file Report, 294 p.
- Back, W., 1960, Origin of hydrochemical facies of ground water in the Atlantic Coastal Plain: 21st International Geological Congress, Copenhagen 1960, Report, pt. 1, p. 87-95.
- Bernard, H. A., and Majors, C. F., Jr., 1963, Recent meanderbelt deposits of the Brazos River: an alluvial sand model: abst. Am. Assoc. Petroleum Geologists Bull., v. 47, no. 2, p. 350
- Bernard, H. A., Major, C. F., Jr., Parrott, B. S., and LeBlanc, R. J., Jr., 1970, Recent sediments of southeast Texas, a field guide to the Brazos alluvial deltaic plains and the Galveston barrier island complex: The University of Texas at Austin, Bureau of Economic Geology, Guidebook 11, 132 p.
- Bishop, R. S., 1978, Mechanism for emplacement of piercement diapirs: American Association Petroleum Geologists Bulletin, v. 62, p. 1561-1583.
- Donaldson, A. C., Martin, R. H., and Kanes, W. H., 1970, Holocene Guadalupe delta of Texas Gulf Coast, in Morgan, J. P., ed., Deltaic sedimentation, modern and ancient: Society of Economic Paleontologists and Mineralogists Special Publication 15, p. 107-137.
- Echols, D. J., and Malkin, D. S., 1948, Wilcox (Eocene) stratigraphy, a key to production: Amer. Assoc. of Petroleum Geologists Bull., v. 32, p. 11-33.
- Fisher, W. L., Brown, L. F., Jr., McGowen, J. H., and Groat, C. G., 1973, Environmental geologic atlas of the Texas Coastal Zone-Beaumont-Port Arthur area: The University of Texas at Austin, Bureau of Economic Geology, 93 p.

Wilcox Group of Texas and their relationship to occurrence of oil and gas: The University of Texas, Bureau of Economic Geology, Geology Circ. 67-4, p. 105-125.

Fisher, W. L., McGowen, J. H., Brown, L. F., Jr., and Groat, C. G., 1972, Environmental geologic atlas of the Texas Coastal Zone-Galveston-Houston area. The University of Texas at Austin, Bureau of Economic Geology, 91 p.

Fogg, G. E., 1980a, Hydrologic stability of Oakwood Dome, in Kreitler, C. W., Agagu, O. K., Basciano, J. M., Collins, E. W., Dix, O., Dutton, S. P., Fogg, G. E., Giles, A. B., Guevara, E. H., Harris, D. W., Hobday, D. K., McGowen, M. K., Pass, D., and Wood, D. H., 1980, Geology and geohydrology of the East Texas Basin, a report on the progress of nuclear waste isolation feasibility studies [1979]: The University of Texas at Austin, Bureau of Economic Geology, Geologic Circular 80-12, p. 30-32.

\_\_\_\_\_ 1980b, Aquifer modeling at Oakwood dome, in Kreitler, C. W., and others, 1980, Geology and geohydrology of the East Texas Basin, a report on the progress of nuclear waste isolation feasibility studies [1979]: The University of Texas at Austin, Bureau of Economic Geology, Geologic Circular 80-12, p. 35-40.

\_\_\_\_\_ 1980c, Regional aquifer hydraulics, East Texas Basin, in Kreitler, C. W. and others, 1980, Geology and geohydrology of the East Texas Basin, a report on the progress of nuclear waste isolation feasibility studies [1979]: The University of Texas at Austin, Bureau of Economic Geology, Geologic Circular 80-12, p. 55-67.

\_\_\_\_\_ 1980d, Salinity of formation waters, in Kreitler, C. W. and others, 1980, Geology and geohydrology of the East Texas Basin, a report on the progress of nuclear waste isolation feasibility studies [1979]: The University of Texas at Austin, Bureau of Economic Geology, Geologic Circular 80-12, p. 68-72.

Fogg, G. E., and Seni, S. J., 1981, A depositional systems approach to groundwater modeling, abst. Geol. Soc. of America Fall 1981 Meeting.

- Kaiser, W. R., 1974, Texas lignite: near surface and deep-basin resources: The University of Texas, Bureau of Economic Geology, Report of Investigation 79, 70 p.
- Kaiser, W. R., Johnston, J. E., and Bach, W. N., 1978, Sand-body geometry and the occurrence of lignite in the Eocene of Texas: The University of Texas at Austin, Bureau of Economic Geology, Geological Circular 78-4 19 p.
- Keys, W. S., and MacCary, L. M., 1971, Application of borehole geophysics to water resource investigations, Chapter E1: U. S. Geol. Survey Tech. Water-Resources Inv., Bk. 2, Chap. E1, 126 p.
- Kreitler, C. W., 1980, Studies of the suitability of salt domes in East Texas Basin for geologic isolation of nuclear wastes: The University of Texas, Bureau of Economic Geology, Geological Circular 80-5, 7 p.
- Kreitler, C. W., Guevara, E., Granata, G., and McKalips, D., 1977, Hydrogeology of Gulf Coast aquifers Houston-Galveston area, Texas: Gulf Coast Assoc. Geological Societies Trans. v. 27, p. 72-89.
- Kreitler, C. W., Agagu, O. K., Basciano, J. M., Collins, E. W., Dix, O., Dutton, S. P., Fogg, G. E., Giles, A. B., Guevara, E. H., Harris, D. W., Hobday, D. K., McGowen, M. K., Pass, D., and Wood, D. H., 1980, Geology and geohydrology of the East Texas Basin, a report on the progress of nuclear waste isolation feasibility studies [1979]: The University of Texas at Austin, Bureau of Economic Geology Geological Circular 80-12, 112 p.
- Kreitler, C. W., and others, in preparation, Geology and geohydrology of the East Texas Basin, a report on the progress of nuclear waste isolation feasibility studies [1980] The University of Texas at Austin, Bureau of Economic Geology Geological Circular

- Galloway, W. E., 1968, Depositional systems of the lower Wilcox Group, North-Central Gulf Coast Basin: Gulf Coast Assn. of Geological Societies Trans., v. 18, p. 275-289.
- Galloway, W. E., 1977, Catahoula Formation of the Texas Coastal Plain: depositional systems, composition, structural development, groundwater flow history and uranium distribution: The University of Texas, Bureau of Economic Geology, Report of Investigations No. 87, 59 p.
- Galloway, W. E., and Kaiser, W. R., 1980, Catahoula Formation of the Texas Coastal Plain: Origin, geochemical evolution and characteristics of uranium deposits: The University of Texas, Bureau of Economic Geology, Report of Investigations No. 100, 81 p.
- Giles, A. B., 1980, Evolution of East Texas salt domes: in Kreidler, C. W., Agagu, O. K., Basciano, J. M., Collins, E. W., Dix, O., Dutton, S. P., Fogg, G. E., Giles, A. B., Guevara, E. H., Harris, D. W., Hobday, D. K., McGowen, M. K., Pass, D., and Wood, D. H., 1980, Geology and geohydrology of the East Texas Basin, a report on the progress of nuclear waste isolation feasibility studies (1979): The University of Texas at Austin Bureau of Economic Geology, Geological Circular 80-12, p. 20-29.
- Henry, C. D., and Basciano, J. M., 1979, Environmental geology of the Wilcox Group lignite belt, East Texas: The University of Texas, Bureau of Economic Geology, Report of Investigations 98, 28 p.
- Jones, L., 1977, Slice technique applied to uranium favorability in uppermost Tertiary of East Texas and West Louisiana: Gulf Coast Association of Geol. Soc. 27th Annual Meeting, p. 61-68.

Kupfer, D. H., 1970, Mechanism of intrusion of Gulf Coast salt, in Geology and Technology of Gulf Coast Salt, a symposium: School of Geoscience, Louisiana State University, p. 25-66.

Loocke, J. E., 1978, Growth history of Hainesville Salt Dome, Wood County, Texas: Unpub. Master's Thesis, The University of Texas at Austin, 95 p.

McGowen, J. H., Brown, L. F., Jr., Evans, T. J., Fisher, W. L., and Groat, C. G., 1976, Environmental geological atlas of the Texas Coastal Zone-Bay City-Freeport area, The University of Texas at Austin, Bureau of Economic Geology, 98 p.

---

Nettleton, L. L., 1934, Fluid mechanics of salt domes: American Association Petroleum Geologists Bulletin, v. 18, p. 1175-1204.

---

Trusheim, F., Mechanism of salt migration in northern Germany: American Association Petroleum Geologists Bulletin, v. 44, p. 1519-1540.

Toth, J., 1972, Properties and manifestations of regional ground-water movements: International Geological Congress, 24th, 1972, Proceedings, p. 153-163.

Woodbury, H. O., Murray, I. B., Picford, P. J., and Akers, W. H., 1973, Pliocene and Pleistocene depocenters, outer continental shelf, Louisiana and Texas: Am. Assoc. Petroleum Geologists Bull., v. 57, no. 12, p. 2428-2439.

APPENDICES

## APPENDIX 1

### Well Listing

Appendix 1 lists the well names and Bureau of Economic Geology reference numbers of wells used in this report. The wells are located in figure 1. Compressed cross sections include wells in section lines A<sub>0</sub>-A<sub>0</sub>' to M-M'; lithostratigraphic cross sections include wells on section lines V-V' to Z-Z'. Oakwood Dome area cross section (V-V') and LETCO wells TOH-2A, TOH-2A0, TOG-1, and TOG-1WS are located in figure 17.

## ETWI APPENDIX L

## CROSS SECTION NUMBERS AND WELL NAMES

CROSS SECTION	#	COMPANY	WELL	COUNTY
A <sub>0</sub> -A <sub>0</sub> '	AA-39-08-302	<u>Overton, ed and W. C. (Richy?)</u>	<u>Ware &amp; Bailey #1</u>	ANDERSON
	AA-34-57-801	<u>Hicks, Lee</u>	<u>Davey, H. A. #A-1</u>	
	AA-38-02-202	<u>Perryman, W. C. &amp; Geo. J. Greer</u>	<u>Forrester, H. L. #1</u>	
	AA-38-03-201	<u>Perryman, W. C. &amp; Leche Oil Co.</u>	<u>Pierce #1</u>	
	AA-38-04-201	<u>Herring Drlg. Co. Inc.</u>	<u>Beard-Herring #1</u>	
	AA-38-04-302	<u>Watburn Oil Co.</u>	<u>Cook, Madison #1</u>	
	AA-34-61-803	<u>Watburn Oil Co.</u>	<u>Holman #1</u>	
	DJ-34-61-902	<u>Talbert &amp; Hughey Drlg. Co. &amp; Gulley</u>	<u>Perkins, T. #1</u>	
	DJ-38-05-302	<u>Chambers-Kilroy &amp; McKnight</u>	<u>Cunningham #1</u>	
	DJ-38-06-102	<u>Delta Drlg. Co.</u>	<u>Sanders, Adeline #1</u>	
A-A'	KA-39-08-401	<u>Basin Operating Co.</u>	<u>1-Carpenter Gas Unit #4</u>	FREESTONE
	KA-39-08-501	<u>Humble Oil &amp; Ref. Co.</u>	<u>Carthright, C. J. #1</u>	ANDERSON
	AA-38-01-601	<u>Texas Trading Co. Inc.</u>	<u>Derden #1</u>	
	AA-38-02-501	<u>Sanders &amp; Murchison</u>	<u>Magee, A. R. #1</u>	
	AA-38-02-502	<u>Texas Co.</u>	<u>Cooper, W. W. #1</u>	
	AA-38-02-601	<u>Texas Co.</u>	<u>Hanks, Dock #1</u>	
	AA-38-03-401	<u>Smith &amp; Smith</u>	<u>Montgomery #1</u>	
	AA-38-03-402	<u>Christie Mitchell &amp; Mitchell</u>	<u>Palmer #1</u>	
	AA-38-03-502	<u>Carter-Gragg Oil Co.</u>	<u>Jaramilla #1</u>	
	AA-38-03-621	<u>Azalea Oil Corp.</u>	<u>Quick #1</u>	
	AA-38-03-601	<u>Spence, Ralph</u>	<u>Overton, R. G. #1</u>	
	AA-38-03-604	<u>McKellar &amp; Tynes</u>	<u>Hall, Ruby #1</u>	
	AA-38-04-422	<u>Graham, Hunt</u>	<u>Elrod, L. et al. #1</u>	
	AA-38-04-425	<u>Humble</u>	<u>Elrod Est. #1</u>	
	AA-38-04-621	<u>Byars, B. G.</u>	<u>McLaurine #1</u>	
	AA-38-04-622	<u>Texas Co.</u>	<u>Petri, A. #1</u>	
	AA-38-05-426	<u>Cougar Petroleum Inc.</u>	<u>Jesse Purvey #1</u>	
	AA-38-05-465	<u>Hankamer, Curtis</u>	<u>Cook, W. L. #1</u>	
	AA-38-05-821	<u>Humble</u>	<u>Todd, W. T. #1</u>	
	AA-38-05-541	<u>Humble</u>	<u>Neches Oil Unit #32 Well #1</u>	
	AA-38-05-539	<u>Humble</u>	<u>Eaton, G. W. #20</u>	
	DJ-38-05-546	<u>Humble</u>	<u>Woolery, J. W. #1</u>	
	DJ-38-05-649	<u>Humble</u>	<u>Carter, H. L. #E-1</u>	
	DJ-38-05-657	<u>Humble</u>	<u>Nays, P. #1</u>	
	DJ-38-05-633	<u>Humble</u>	<u>McDougal, M. T. #3</u>	



## ETWI APPENDIX

## CROSS SECTION NUMBERS AND WELL NAMES

CROSS SECTION	#	COMPANY	WELL	COUNTY
-C'	KA-39-15-303	Humble	Bonner, T. R. #1	FREESTONE
	KA-39-16-201	Clay, Thomas W. & Beckman Inc.	Young, Hattie	ANDERSON
	KA-39-16-203	Byars, B. E. et al.	Young, T. F. #1	
	AA-38-10-222	Humble	Hudson, H. L. #B-1	
	AA-38-10-201	Texas Co.	Holmes, M. T. #1	
	AA-38-11-122	Cape Operating Co.	Vance #1	
	AA-38-11-104	Broyles, Gordon B. & J. W. McFarlane	Willhite, T. A. #2	
	AA-38-11-102	La Rue	Jennigan-1	
	AA-38-11-203	La Rue, E. B. Jr. & F. R. Jackson	Scott, Nathan #1	
	AA-38-11-322	Frost, Jack et al.	Walker, Connie Lee #1	
	AA-38-11-301	Perryman, W. C.	Royal Nat'l Bank #1	
	AA-38-12-104	Peveto, R. S.	Barrett W. H. Est. #1	
	AA-38-12-102	Johnson, T. J.	Barnett, Ophelia #1	
	AA-38-12-321	Katz, Sid Expl. & Holly Dev. Co.	McDonald, Mrs. #1	
	AA-38-12-322	Phillips, Loyce	Yates, J. W. #1	
	AA-38-13-121	Lecuno Oil Corp.	Ward, Homer #1	
	AA-38-05-705	Ridley, Locklin & Frank Agar	Davis, N. O. #1	
	AA-38-13-101	General American Oil Co.	Caldwell, John #1	
	AA-38-13-221	Phillips, Loyce	Ballard, Bell #1	
	AA-38-05-852	Humble	Douglas, L. B. #1	
	AA-38-05-853	Humble	Neches Unit #29, Well #1	CHEROKEE
	DJ-38-05-825	Sullivan, Hugh E. et al.	Neches Unit #2, Well #1	
	DJ-38-05-923	American Liberty Oil Co.	Austin, Jeff #1	
	DJ-38-13-301	Texaco	Holman Unit #1	
	DJ-38-14-121	Gey Crude	Black-1	
	DJ-38-14-201	Greiling, L. A.	Batton, O. O. #1	
	-E'	KA-39-16-702	John B. Stephens Jr.	J. W. Brown #1
KA-39-24-301		M. B. Rudman-Dorfman Prod. Co.	Emma Hill #1	ANDERSON
KA-39-16-901		Johnson & Gist	Keys #1	
KA-39-24-201		E. B. LaRue Jr. & W. C. Windsor	R. Steward #1	
AA-38-10-702		Continental	Royal Nat'l Bank #1-A	
AA-38-10-801		J. G. Walker Jr. et al.	F. W. & J. C. Huffman #1	
AA-38-10-622		Devon Leduc	J. H. Barrett #1	
AA-38-11-701		Olson Brothers Inc.	W. A. Jordan #1	
AA-38-11-821		J. R. Miller & J. G. Walker	M. L. Coble #1	





## ETWI APPENDIX

## CROSS SECTION NUMBERS AND WELL NAMES

CROSS SECTION	#	COMPANY	WELL	COUNTY
H-H'	KA-39-24-802 KA-39-24-905 KA-38-17-703 KA-38-17-802 KA-38-17-804 KA-38-17-805 KA-38-17-807 KA-38-18-822 AA-38-18-929 AA-38-18-964 AA-38-19-726 AA-38-19-729 AA-38-19-803 AA-38-19-804 AA-38-19-903 AA-38-19-902 AA-38-20-702 AA-38-20-803 AA-38-20-802 AA-38-20-905 AA-38-20-901	Humble Humble T. J. Johnson et al. Roger Steward Humble Lecuno Oil Corp. Carter-Gragg Oil Co. Jack Frost & R. L. Peveto Kent D. Diehl et al. E. L. Howard & Cooper Carter-Gragg Oil Co. F. R. Jackson & Sam B. King J. L. Gulley Jr. Carter-Gragg Oil Co. S. A. Cochran Happy Gist Johnson & Gist James Fair W. H. Bryant Eugene Talbert & Globe Drlg. Co. C. R. Epperson et al.	W. L. Burgher #1 Red Lake GU #3, Well #1 C. E. Childs #1 Mary Harris #1 1-Butler GU #2 E. Tx. Nat'l Bank Palestine #1 Robert Mims #1 Carter-Gragg #1 Sally Rucker #1 #2 Carter #3 Elizabeth Morrow E. P. Murray et al. #1 C. C. Nivens #1 Davey-Monnig #1 Farris #1 Wilson #1 Madox #1 Fincher #1 Minnie Belle Denson #1 R. B. Fincher #1 C. W. Moore Oil Unit #1	ANDERSON
I'I'	KA-39-32-102 KA-39-32-202 KA-39-32-204 KA-39-32-301 KA-38-25-201 KA-38-25-203 KA-38-25-301 KA-38-25-302 AA-38-18-952 SA-38-27-103 SA-38-27-102 AA-38-27-202 AA-38-27-203 AA-38-27-301	Humble Humble The Atlantic Ref. Co. O. V. Killan Humble Humble Humble Hunt Graham & E. L. Howard Stroube & Stroube Gibson Drlg. Co. et al. Gibson Drlg. Co. & O. L. Gragg Humble Goldston Oil Co. J. R. Meeker et al.	M. E. Gehrels et al. #1 A. W. George #1 Ben Clary #1 Yeager #1 Greer Bros. #C-1 Greer Bros. #1 Butler GU #5 Mary Britton et al. #1 J. O. & H. Monning #6 B. Reeves #1 Coleman Carter #1 J. G. McLen #1 Parrish #1 A. B. Warren #1	FREESTONE          ANDERSON LEON  ANDERSON



## ETWI APPENDIX

## CROSS SECTION NUMBERS AND WELL NAMES

ROSS SECTION	#	COMPANY	WELL	COUNTY	
K'	KA-39-31-701	Humble	R. Eppes #1	FREESTONE	
	KA-39-31-901	Fred H. Garret & T. J. Johnson	G. C. Blair #1	LEON	
	SA-39-40-301	J. W. McFarlane & Gordon B. Broyles	J. W. Henson & Z. A. Rosenthal #1		
	SA-39-40-302	G. M. Jordan	H. P. Van Winkle #1		
	SA-39-40-303	Charles B. Marino	Harrington #1		
	SA-38-25-828	Roger Steward	J. C. Keils #1		
	SA-38-25-902	P. J. Lake Inc.	Leon Plantation #1		
	SA-38-26-706	Humble	SW Oakwood GU #11, Well #1		
	SA-38-26-801	Armstrong	Moore #1		
	SA-38-26-901	Azalea Oil Corp.	C. W. DeVaughn Est. #1		
	AA-38-27-702	Clark & Gabriel	Moore #1		ANDERSON
	AA-38-27-802	Coats Drlg. Co.	O. L. Lively	HOUSTON	
	PA-38-27-902	E. R. Jackson	A. P. Matthews		
	PA-38-28-702	Trice Prod. Co.	B.S. Mathews #1		
	PA-38-28-703	T. D. Humphrey & Sons	Joe A. Brown #1		
	PA-38-28-801	Basin Operating Co., Otd.	H-F-J #1		
	PA-38-28-901	Lecuno Oil Corp.	D. S. Clark #1		
	PA-38-29-701	F. B. Jackson Jr.	Edge #1		
	PA-38-29-901	T. D. Humphrey & Sons Ltd.	Elliot #1		
	PA-38-30-701	Group Oil Co., Wise Drlg. Acc. & Ralph Spence	J. D. Sloan #1		
PA-38-30-801	J. Robert Phillips Jr.	Dr. G. J. Hays #2			
L'	SA-39-40-306	Frank & George Frankel	N. M. Cochran #1	LEON	
	SA-38-33-203	Murray & Mitchell	Pearlstone Recknor #1		
	SA-38-33-301	Gulley Drlg. Co.	McBrayne #1		
	SA-38-33-303	Humble	SW Oakwood GU #2, Well #1		
	SA-38-34-121	Humble	SW Oakwood GU #3		
	SA-38-34-104	Humble	SW Oakwood GU #6, Well #1		
	SA-38-34-201	American Liberty Oil Co.	Thrash #1		
	SA-38-34-302	Union Oil Co. of Calif.	Gertrude Rennoe et al. #1		
	PA-38-35-101	English Jackson Jr. & Johnson Drlg. Co.	F. P. McCall Estate #1		HOUSTON
	PA-38-35-201	Sid Katz Expl. & R. E. Smith	W. L. Moody Est. #1		
	PA-38-35-301	The New Seven Falls Co.	Bettie Jones et al. #1		
	PA-38-35-302	F. R. Jackson	Dailey #1		



## APPENDIX 2

### Data from LETCO Wells TOH-2A and TOH-2A0

Appendix 2 includes a detailed lithologic description, lithologic log, and grain-size data from LETCO core hole TOH-2A0 and geophysical logs (gamma ray, self potential, and induction resistivity (ILD)) from LETCO core hole TOH-2A. The two holes are approximately 15 m (50 ft) apart. Core descriptions were logged by examination of slabbed core sections with a hand lens and binocular microscope. The color, composition, structures, texture, and constituents were recorded on a log form at a scale of 5 ft to 1 inch. Data on the occurrence of glauconite was from petrographic analysis of thin sections. Mean grain size ( $M_z = \frac{016 + 050 + 084}{3}$ ) of samples from TOH-2A0 was measured on a rapid sediment analyzer for the sand-sized fraction and on a coulter counter for the silt and clay fraction. The mean grain size is applicable only to extrabasinal grains (quartz and other labile grains). The grain size was not measured for sedimentation units composed primarily of intrabasinal mudclast sand and gravel due to problems with destruction of soft grains during disaggregation and with the large maximum grain size (up to 5 cm). Geophysical logs from TOH-2A are displayed in parallel with data from TOH-2A0 but are for reference only because of the possibility of lithologic changes over the area between the two wells.

## CORE DESCRIPTION OF WILCOX GROUP Letco TOH-2A0

Depth (ft' below surface)	Recovered Core (ft)	
500 - 560	2	2 feet silt, and clay, dark gray, parallel laminated, wavy and ripple cross-laminated.
560 - 620	2	1 foot fine sandstone, green, glauconitic, clayey, unconsolidated 1 foot of claystone, gray, structureless.
620 - 640	5	5 feet medium sandstone, gray, soft, partly structureless with some inclined laminae; fine sand and clay parallel laminated at base.
642.5 - 678	30	30 feet very fine sandstone, medium gray and greenish gray, parallel and incline laminated, locally clayey; parallel laminated with silt and silty clays, wavy and ripple cross-laminated few small scale trough cross-laminations, occasional clay granules. Some fissile shale breaks are present with some organic matter throughout. The basal 1 foot claystone, lignitic
685 - 720	11.5	11.5 feet clayey siltstone, light gray soft, thinly laminated with very fine sand. Foundered ripple sets and parallel inclined laminations, some convolute laminae at top.
720 - 743	23	23 feet silty very fine sandstone, light gray, parallel laminated with clayey siltstone and shale laminae, parallel laminated and ripple cross-laminated.
743 - 789	46	46 feet fine sandy flat pebble (mud clast) conglomerate, tan, light to medium gray, individual beds 4 in to 9 ft thick silty and clayey in parts, soft and thinly interbedded with mottled silty claystone and shale, parallel laminated, fissile, some folding or slump features present.

## CORE DESCRIPTION OF WILCOX GROUP Letco TOH-2A0

Depth (ft below surface)	Recovered Core (ft)	
790 - 807.7	17.7	17.7 feet fine sandstone, light gray, thinly interbedded with clayey sandstone and sandy clay, parallel laminated with abundant disseminated carbonaceous matter.
824 - 841.5	17.6	17.5 feet siltstone and shale, medium gray, thinly interbedded and interlaminated with common ripple cross laminae - few pebbles, rare parallel inclined laminations.
841.5 - 909.5	60	60 feet fine sandstone, whitish gray to medium gray, interlaminated with clayey sands and shale, common ripple cross and parallel inclined laminations, locally structureless, rare mud clast pebbles; locally abundant lignitic matter in beds 0.5 to 6.0 in thick; fractured, some clay-filled; pyrite spheres present granule sized.
910 - 939	29	29 feet and very fine and fine sandstone, grayish white to dark gray, interlaminated with clayey sand containing few ripple cross and parallel inclined laminae. Flat pebble conglomerate locally present; upper two feet calcite cemented, pyritic.
939 - 955	14	14 feet very fine sandstone, light gray, interlaminated with silty and sandy claystone and flat pebble conglomeratic very fine sandstone.
955 - 989	27	27 feet clayey siltstone, dark gray to greenish gray, interlaminated silty claystone, wispy, parallel laminated and ripple cross laminated; pyrite is very common.

## CORE DESCRIPTION OF WILCOX GROUP Letco TOH-2A0

Depth (ft below surface)	Recovered Core (ft)	
989 - 999	12.5	12.5 feet claystone, black to dark gray, lignitic, wispy laminated silty at base, blocky fracture.
999 - 1004.5	5.5	5.5 feet siltstone, clayey wavy laminated with small sets (0.5-1 in) of ripple cross laminae and clay stringer (0.5-1 in) at base.
1004.5 - 1040	35.5	35.5 feet very fine sand, medium gray, interlaminated silty sand, sandy clays and clays; <sup>fine sandy</sup> flat pebble conglomerate, 0.3 to 3 cm beds, carbonaceous, wispy laminated and ripple cross-laminated; disturbed bedding.
1040 - 1063	23	23 feet silt, silty clay, and clayey silt, gray, thinly laminated disseminated carbonaceous matter; silts, wispy to parallel laminated, abundant ripple cross laminations; very fine sandstone and clay pebble conglomerate is rare.
1063 - 1075.5	10.5	10.5 feet sandy claystone, medium gray, interlaminated siltstone, and shale, fissile; wispy laminated; common laminae of macerated carbonaceous debris.
1075.5 - 1101.5	14	14 feet sandy claystone, medium gray, interlaminated siltstone and shale, wispy laminated, ripple cross laminated, burrowed, common laminae of macerated carbonaceous debris; 0.5 ft bed of fine sandy mudclast granule conglomerate.
1101.5 - 1115	4	4 feet very fine sandstone, dark brown (wet), parallel laminated, wispy laminated with sandy clay.

## CORE DESCRIPTION OF WILCOX GROUP Letco TOH-2A0

Depth (ft below surface)	Recovered Core (ft)	
1137.5 - 1141	3.5	3.5 feet siltstone, gray, bioturbated, interlaminated with clayey silts, wispy and parallel laminated.
1157 - 1170	13	13 feet silty very fine sandstone, brownish gray, calcitic interlaminated and interbedded with silty clays, siltstone; wavy, wispy and ripple laminations common; disturbed bedding occurs in the calcite cemented sandstone.
1170 - 1183.5	2.5	2.5 feet claystone, black, lignitic, locally fissile.
1183.5 - 1188	4.5	4.5 feet clayey fine sandstone, tan to gray, burrowed, parallel laminated at base, common disseminated carbonaceous matter.
1202 - 1255	53	53 feet silty claystone, light, medium, and dark gray, patchy calcitic cement, interlaminated with siltstone, and shale, commonly rooted, mottled and with macerated carbonaceous matter, silts and clayey silts bioturbated also parallel and ripple cross laminated; inclined parallel laminations and disturbed bedding is present, occasional pyritic patches.
1260 - 1264	4	4 feet very fine sandstone, gray, ripple cross-laminated, interbedded with mudclast pebble conglomerate and interlaminated silts and silty clays.
1266.5 - 1294	20	20 very fine sandstone, light gray, calcitic, interlaminated clayey sand, ripple cross-laminated, some disturbed bedding in calcite cemented areas; few granules and pebbles of lignite, mudstone and sandstone present.

## CORE DESCRIPTION OF WILCOX GROUP Letco TOH-2A0

Depth (ft below surface)	Recovered Core (ft)	
1294 - 1344	50	50 feet fine sandy siltstone, light gray, interlaminated with silty clays and occasional fissile shale laminae, ripple cross-laminated and contorted bedding (slump) common, inclined parallel laminae at base.
1344 - 1355	11	11 feet silty claystone, gray predominately structureless, clayey siltstone at base.

## CORE DESCRIPTION OF WILCOX GROUP Letco TOH-2A0

Depth (ft. below surface)	Recovered Core (ft)	
1360 - 1388	28	shaley siltstone 28 feet shale, interlaminated with medium gray, calcitic, fissile, bioturbated, and ripple cross-laminated
1388 - 1399	11	11 feet clayey siltstone, medium gray, interlaminated with silty clay and silty very fine sandstone, ripple cross-laminated, bioturbated.
1410 - 1425	12	12 feet claystone and shale, light to medium gray, calcitic, bioturbated, interlaminated with siltstones.
1425 - 1448	15.5	15.5 feet very fine sandstone, light gray, structureless to parallel laminated, thinly interbedded with clayey sandstone, burrowed zone may contain dead oil stain.
1449 - 1456.5	4	4 feet sandy clayey siltstone, carbonaceous, bioturbated, ripple cross-laminated, and structureless.
1456.5 - 1459	2.5	2.5 feet very fine sandstone, grayish brown, lignite bed very carbonaceous, 3-inch thick, common lignite fragments; may have an oil stain.
1460 - 1477.5	15	15 feet fine sandstone, light gray, structureless, parallel and thinly interbedded with clayey and silty fine sandstone, rare medium sandstone, wispy and disturbed bedding present; basal part very fine sandstone, silty, carbonaceous.

## CORE DESCRIPTION OF WILCOX GROUP Letco TOH-2A0

Depth (ft below surface)	Recovered Core (ft)	
1477.5 - 1489	12.5	12.5 feet very fine sandstone, medium gray, calcitic, carbonaceous, interlaminated with clayey sandy silts, ripple cross-laminated, highly bioturbated
1489 - 1498	9	9 feet shale, medium gray, fissile, burrowed and slightly calcitic with some thin lignite layers.
1498 - 1529	31	31 feet siltstone, gray, parallel laminated with clayey silts, silty clays, and very fine sandstone, bioturbated, with some patchy calcite nodules; abundant lignitic clay, black.
1529 - 1575.5	37	37 feet silty claystone, light to medium gray, bioturbated and structureless with few parallel laminations and fissile shale; common lignitic clay, black.
1575.5 - 1585	9.5	9.5 feet sandy siltstone, greenish gray, interbedded with silty clay, structureless; common lignitic clay, black.
1585 - 1592	7	7 feet silty very fine sandstone, gray, interlaminated with fine to medium sandstone, poorly sorted, parallel and wavy laminated, ripple cross-laminated.
1625 - 1631	6	6 feet fine sandstone, whitish gray, structureless, moderately sorted, common disseminated carbonaceous matter.

## CORE DESCRIPTION OF WILCOX GROUP Letco TOH-2A0

Depth (ft below surface)	Recovered Core (ft)	
1631 - 1645	14	14 feet shaley siltstone, gray, locally slightly calcitic, wavy laminated and burrowed, thin laminae of medium sandstone, structureless.
1645 - 1684.5	16.5	16.5 feet silty claystone, medium gray, calcitic, wavy and ripple cross-laminated, light greenish gray at base.
1684.5 - 1685.5	1	1 foot orange-brown medium sandstone, hard, limonitic, parallel inclined and ripple cross-laminated.
1685.5 - 1708	20.5	20.5 feet silty claystone, medium to dark gray, hard, locally carbonaceous with occasional lignite and rooted lignitic clays.
1708 - 1719.5	11.5	5.5 feet clayey, very fine sandstone, medium gray, carbonaceous and ripple cross-laminated overlying 6 feet fine sandy siltstone, interlaminated with silty clay, bioturbated, orange-brown stained, ripple cross-laminated.
1719.5 - 1738	15.5	15.5 feet silty claystone, whitish gray to dark gray, locally lignitic, rooted and bioturbated, wavy and ripple cross-laminated.
1738 - 1743	5	5 feet clayey siltstone, brownish gray, bioturbated, wavy and ripple cross-laminated.

## CORE DESCRIPTION OF WILCOX GROUP Letco TOH-2A0

Depth (ft below surface)	Recovered Core (ft)	
1743 - 1753.5	7.5	7.5 feet very fine sandstone, medium gray, inter-laminated silty clays, locally bioturbated, blocky, ripple cross-laminated, common disseminated carbonaceous matter.
	1.5	1.5 feet lignite, black, subfissile.
1791 - 1831	40	40 feet clayey siltstone, medium to dark gray, rooted and interlaminated with shales and silty clays, slightly calcitic, locally carbonaceous, inclined abundant ripple cross-laminations, common parallel and wavy laminations, locally bioturbated, few rootlets, rare parallel laminae; lower 3 feet shale and interbedded siltstones.
1831 - 1836	5	5 feet silty very fine sandstone, light gray, ripple cross-laminated with small-scale, 1 to 2 inch trough-fill cross-laminated.
1837 - 1852	10	10 feet siltstone, medium to dark gray, calcitic, interlaminated silty clays, very fine sandstone, and shale, wispy and ripple cross-laminated.
1852 - 1883	27	27 feet shale, medium to dark gray, interlaminated lignite and silty claystone, rooted and bioturbated, wispy laminated.

## CORE DESCRIPTION OF WILCOX GROUP Letco TOH-2A0

Depth (ft below surface)	Recovered Core (ft)	
1883 - 1896	13	13 feet shaley siltstone, medium to dark gray, bio-turbated, interlaminated fine to medium sandstone and shale, wispy and ripple cross-laminated, common scour surfaces bear unknown brown mineral.
1896 - 1903	5	5 feet shale, light to medium gray, slightly calcitic.

## CORE DESCRIPTION OF WILCOX GROUP Letco TOH-2A0

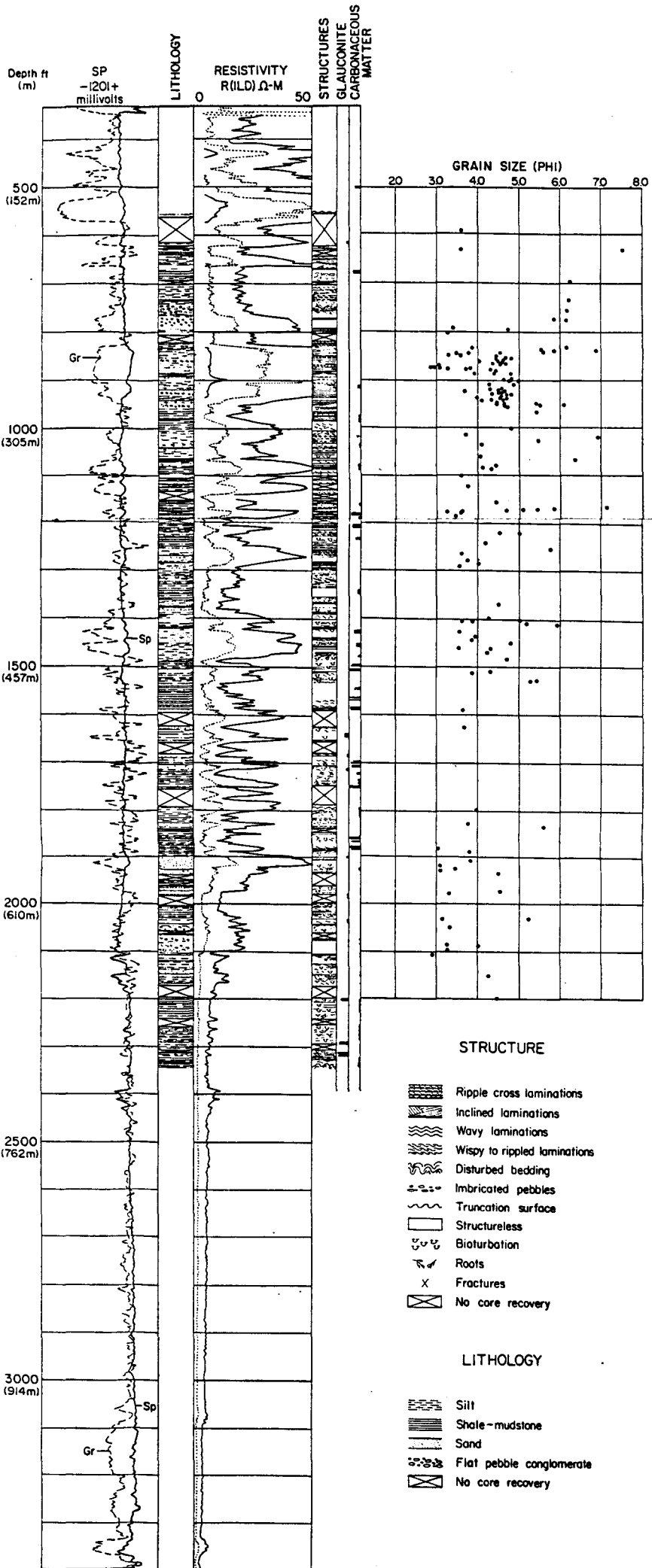
Depth (ft below surface)	Recovered Core (ft)	
1903 - 1909	6	6 feet very fine sandstone, light gray, carbonaceous, wispy and ripple cross-laminated, few shale laminations.
1911 - 1925.5	14	14 feet fine sandstone, yellow to medium gray, limonitic poorly sorted, soft and structureless, some burrows at base.
1925.5 - 1929	2.5	2.5 feet clayey siltstone and shale, dark gray, fissile.
1929 - 1938.5	9.5	9.5 feet clayey very fine sandstone, medium gray, wispy and ripple cross-laminated, few shale laminations, common disseminated carbonaceous matter.
1956.5 - 1959	25	25 feet clayey siltstone, dark gray, common silt-filled burrows and few wispy laminations.
1966 - 1982	16	16 feet clayey very fine sandstone, light gray, inter-laminated with silty clays, dark-gray, wispy laminated, abundant bioturbation.
1986 - 1988	2	2 feet shale, dark gray, fissile.
2006 - 2021	15	15 feet siltstone, gray, calcitic, interlaminated, shale and silty clays, parallel laminated, some wispy laminations, pyritic, silt-filled burrows common.
2026 - 2034.5	10	10 feet siltstone, light gray, calcitic, interbedded shale, silty clays, and very fine sandstone, pinkish brown, parallel laminated, some wispy laminations.
2034.5 - 2052.5	14	14 feet clayey, very fine sandstone, light gray, thinly interbedded with shale, dark gray, fissile, common disseminate carbonaceous matter.
2052.5 - 2099	30.5	30.5 feet very fine sandy mudclast granule to pebble conglomerate, light gray, structureless, interbedded with granular very fine sandstone, structureless, thinnly interbedded with shale, rare parallel laminations and burrows.

## CORE DESCRIPTION OF WILCOX GROUP Letco TOH-2A0

Depth (ft below surface)	Recovered Core (ft)	
2099 - 2103	4	4 feet fine sandstone, structureless.
2107 - 2111.5	4.5	4.5 feet silty shale, black, fissile.
2111.5 - 2119	7.5	7.5 feet silty very fine sandstone and sandy siltstone, parallel and ripple cross-laminated, with some calcite-cemented nodules.
2127 - 2150.5	23.5	23.5 feet shale and siltstone, gray, calcitic interlaminated, abundantly wispy laminated, inclined and ripple cross-laminated, bioturbated.
2150.5 - 2169.5	19	19 feet shale and siltstone, gray calcitic, interlaminated, very fine sandstone, interbedded 0.3 to 3.0 feet thick, parallel and wispy laminated, disturbed bedding in very fine sandstone.
2169.5 - 2170	0.5	Siderite nodule, brown, hard, sand-filled burrows, glauconitic.
2201.5 - 2208.5	7	7 feet siltstone, brownish-gray, slightly greenish, thinly interbedded with shale, very glauconitic, silt and glauconite-filled burrows, ripple cross-laminated and carbonaceous.
2212 - 2235	23	23 feet shale, medium to dark gray, locally slightly calcitic, subfissile, thinly laminated with silty clays, common disseminated carbonaceous matter, burrowed.
2235 - 2266	12	12 feet shale, medium to dark gray, locally slightly calcitic, interbedded with siltstone, light gray to tan, moderately indurated, parallel and ripple cross-laminated to structureless.

## CORE DESCRIPTION OF WILCOX GROUP Letco TOH-2A0

Depth (ft below surface)	Recovered Core (ft)	
2266 - 2290	24	24 feet shale and siltstone, light and medium gray, thinly interbedded and interlaminated common disseminated carbonaceous matter, extensively bioturbated.
2290 - 2314.5	13.5	13.5 feet shale and silt, light and medium gray, thin laminations of siltstone, whitish-gray, locally glauconitic.
2314.5 - 2320	5.5	5.5 feet sandy siltstone, greenish-gray, glauconitic, parallel and slightly incline laminated, extensively burrowed, 1.5 feet thick, siltstone, reddish-brown, ripple cross-laminated.
2320 - 2348	28	28 feet shale and silts, medium to dark gray, interlaminated carbonaceous, blocky to subfissile, parallel laminated, ripple cross-laminated silt-filled burrows, locally bioturbated, disturbed bedding.
		END OF CORE.



## APPENDIX 3

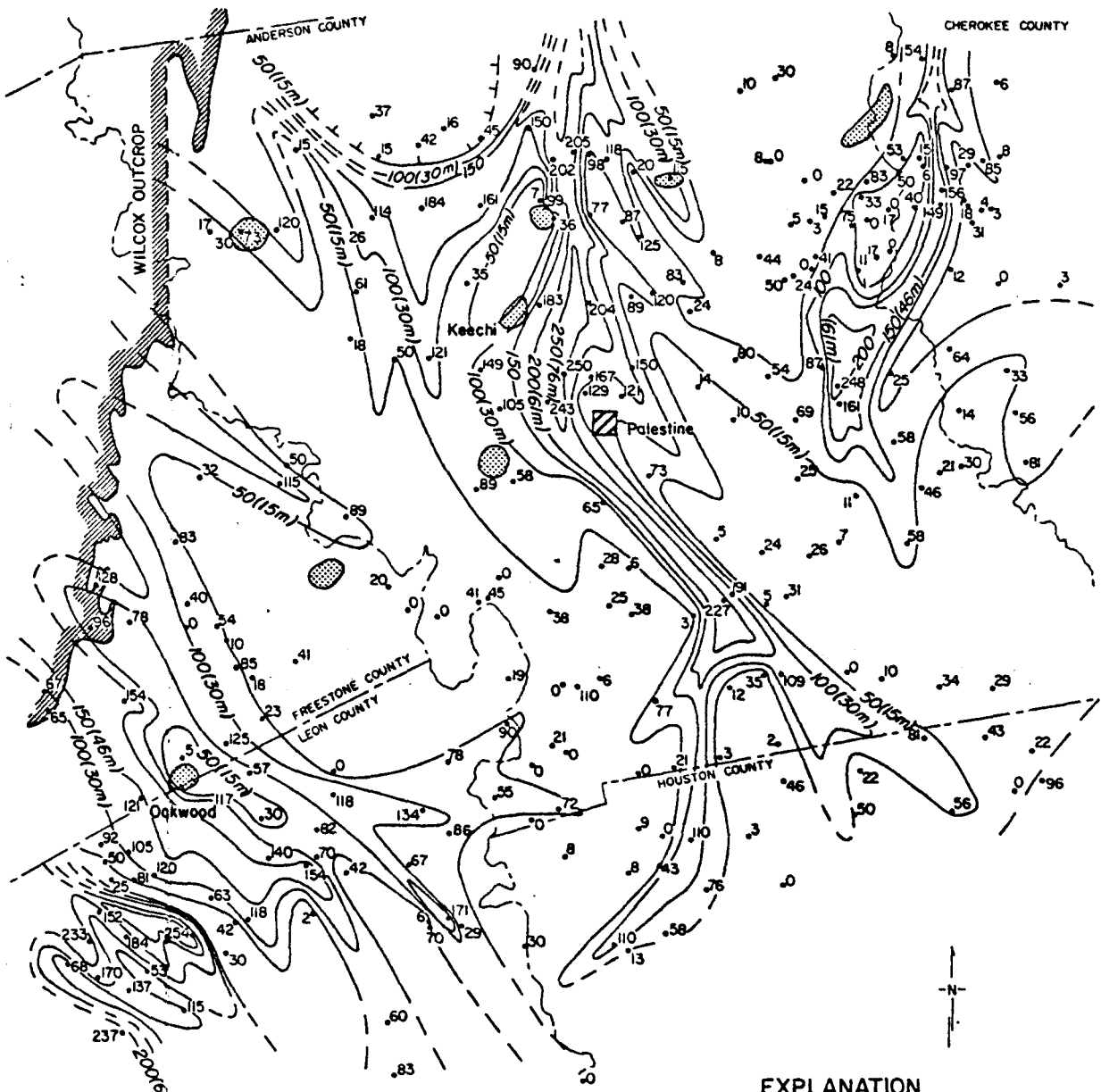
### Net and Percentage Maps

Appendix 3 includes net and percentage maps of sandstone greater than 200m. The Wilcox was divided into three layers of equal thickness. The purpose was to understand vertical as well as lateral variations in sandstone distribution. By limiting the vertical thickness and time required to deposit the / <sup>strata</sup> represented in a single map layer, the trends mapped are much sharper than if the undivided / <sup>Wilcox</sup> were mapped. The three-fold division mimics, in part, the three-fold stratigraphic division of the Wilcox into the Hooper, Simsboro, and Calvert Bluff Formations. In the eastern part of the study area, the Simsboro Formation is lost as a mappable unit, thus the necessity of an arbitrary division.

Both net and percentage sandstone (greater than 200m) maps were constructed for each layer. Little variation is evident between the two map sets because the thickness of the Wilcox is not extremely variable in the study. In the vicinity of the outcrop belt erosion has truncated the Wilcox. A coalescence of sandstone trends may be due to this truncation or due to / <sup>the</sup> invasion of recharging, resistive meteoric ground water.

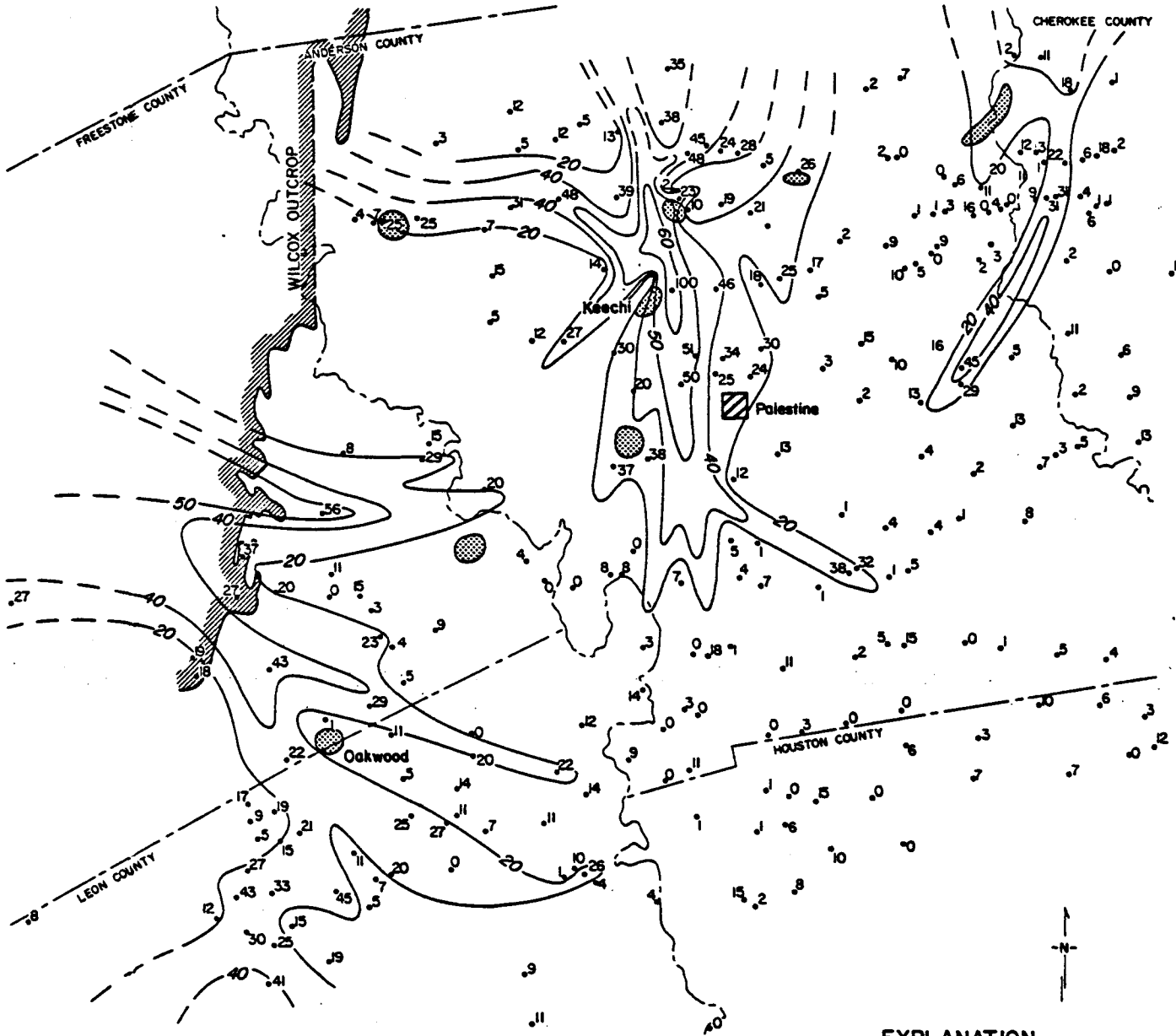
Facies maps were developed for each layer from the net sandstone maps. Channel facies are outlined by dip-oriented sandstone (greater than 200m) belts with greater than 30 m (100 ft) sandstone (greater than 200m). For the lowest or first layer the change from dip-oriented belts to lobate sheets signifies the change from fluvial channel to deltaic facies. Interchannel facies occur in the fluvial system over areas with less than 30 m (100 ft) net sandstone (greater than 200m). The middle map layer is entirely fluvial as the dip-oriented belts extend across the

study area. The middle layer contains the greatest amount of sandstone. The upper layer is mud-rich and is analogous to the Calvert Bluff Formation.



**EXPLANATION**  
 ● Salt dome  
 Contour interval = 50ft  
 Upper layer ~~is~~ <sup>not</sup> Sandstone > 200m

*J. Adams*  
*Jan 1977*

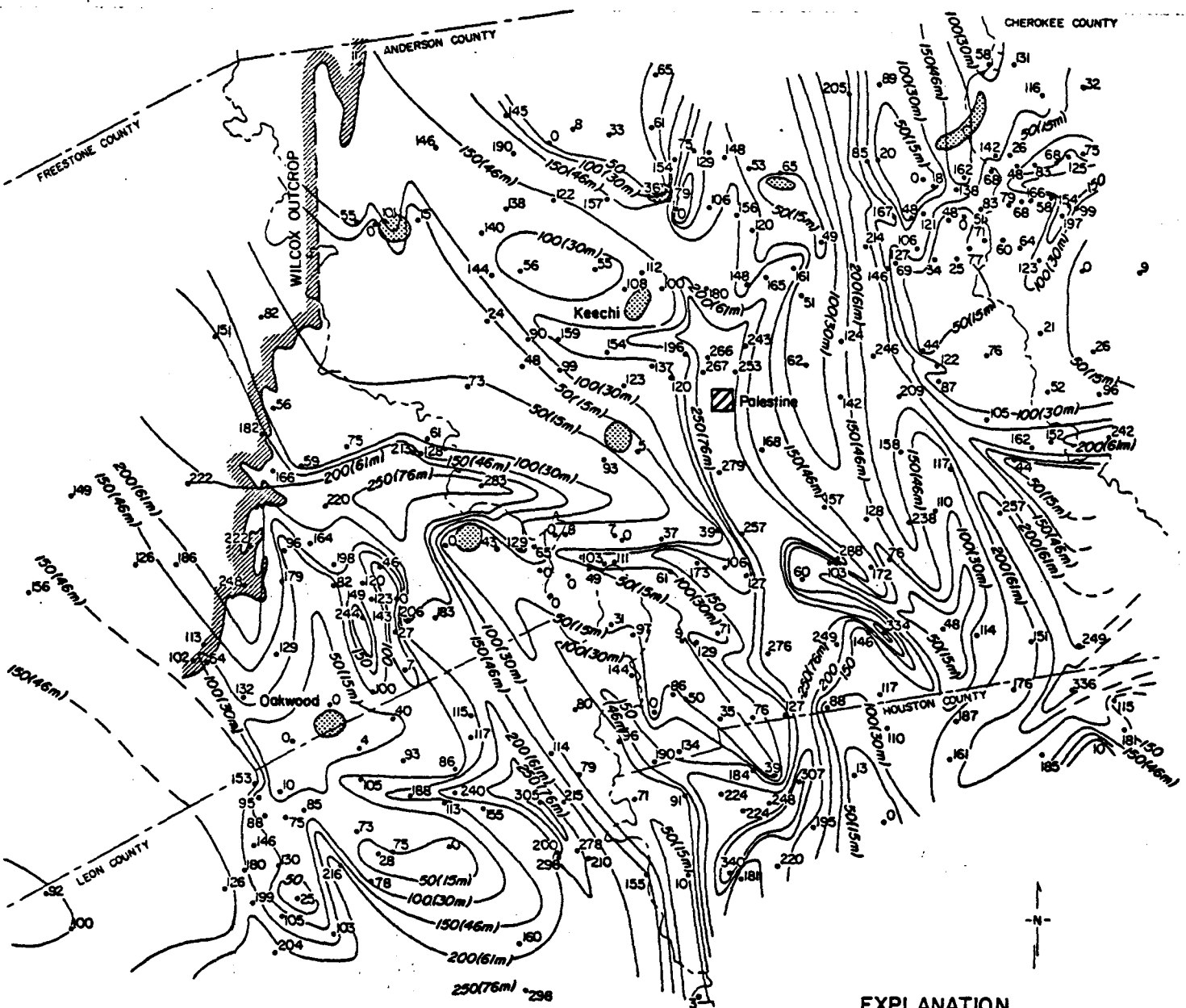


**EXPLANATION**

-  Salt dome
- Contour interval = 10-20%

*Upper Layer Percent Salt at 720m*

*[Faint handwritten notes and scribbles at the bottom of the page]*



**EXPLANATION**

-  Salt dome
- Contour interval = 50ft

*Middle layer Net Sand stone > 20.0 m*

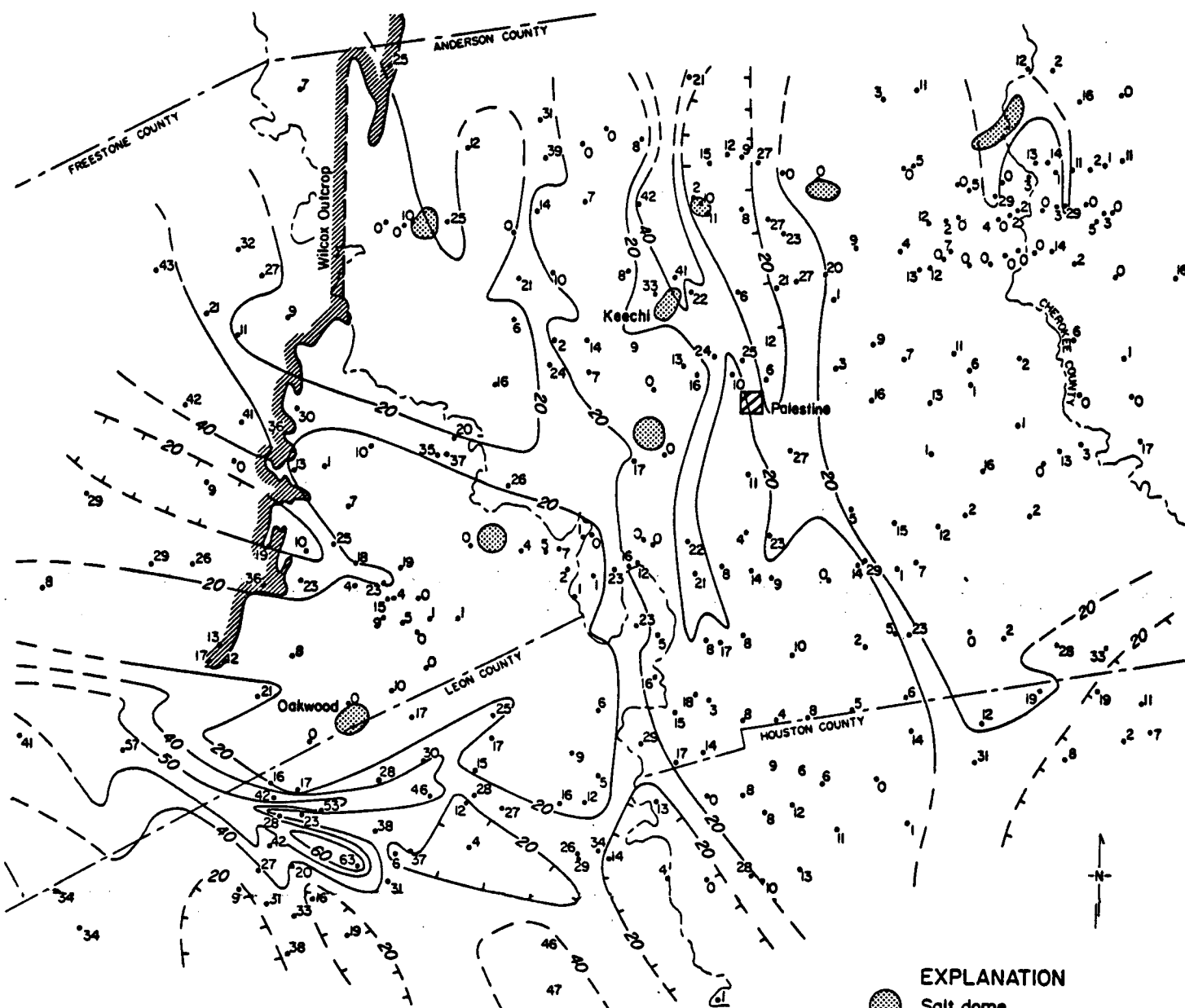


Middle Layer Percent Sandstone 7205-11



**EXPLANATION**  
 ● Salt dome  
 Contour interval = 50ft

*Lower layer No. Sandstone > 20.0m*



**EXPLANATION**  
 ● Salt dome  
 Contour interval = 10-20'

*Lower layer forant Saltsome > 200m*

## APPENDIX 4

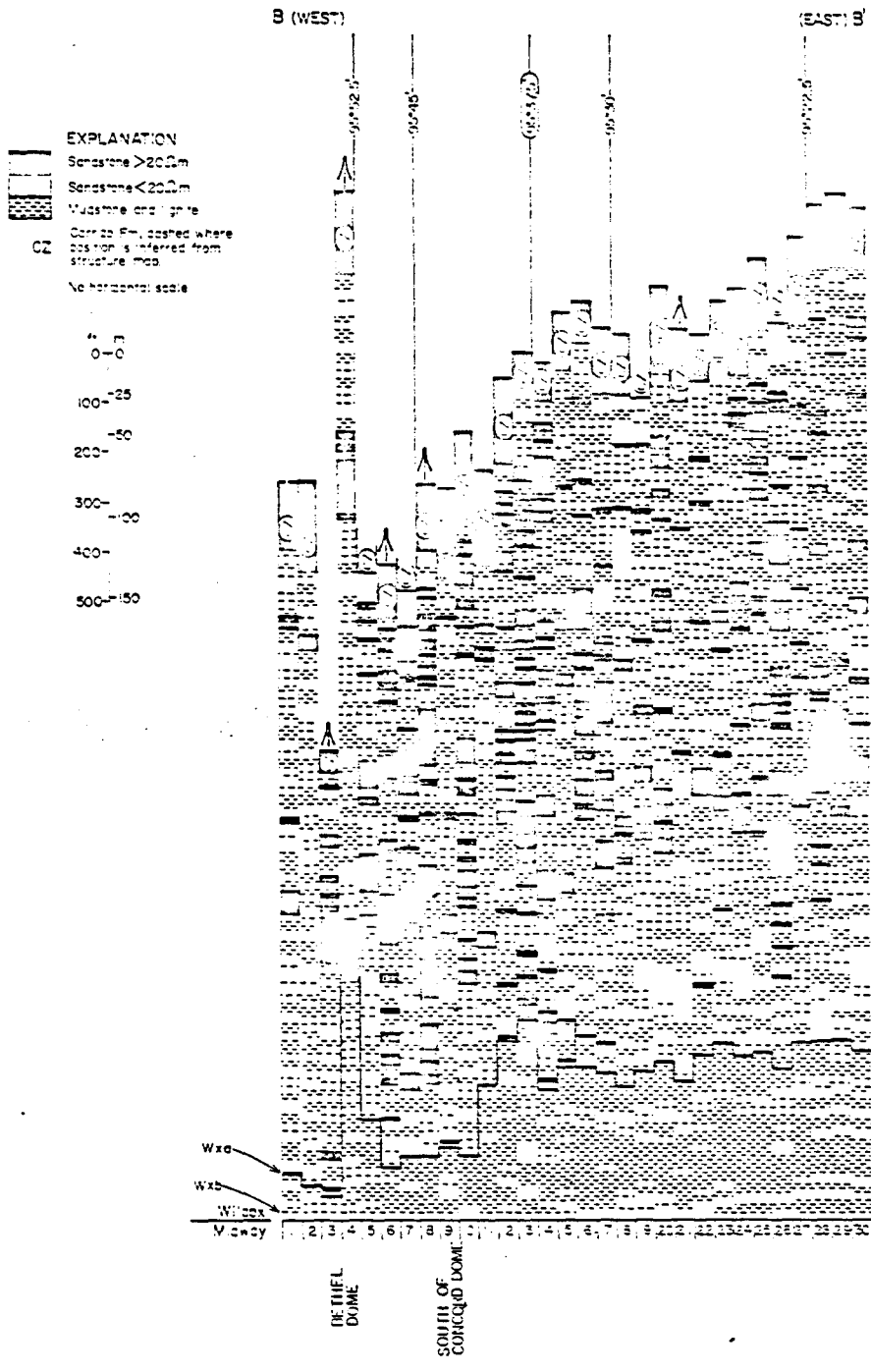
### Compressed Cross Sections

Compressed sections B-B', E-E', F-F', G-G', I-I', K-K', and M-M' are presented in Appendix 4. Compressed cross sections evolved from lithostratigraphic cross sections and the requirements of computer modeling of ground-water flux. The position, distribution, and geometry of sandstones with high hydraulic conductivities (permeabilities) is much more important for purposes of ground-water modeling than similar data on thin, hydrologically isolated sandstones.

Facies mapping (Appendix 3) was restricted to sandstones with induction log (ILD) measured resistivities greater than  $20\ \underline{\mu}\text{m}$ . These sandstones have hydraulic conductivities one to three orders of magnitude greater than sandstones with resistivities less than  $20\ \underline{\mu}\text{m}$ .

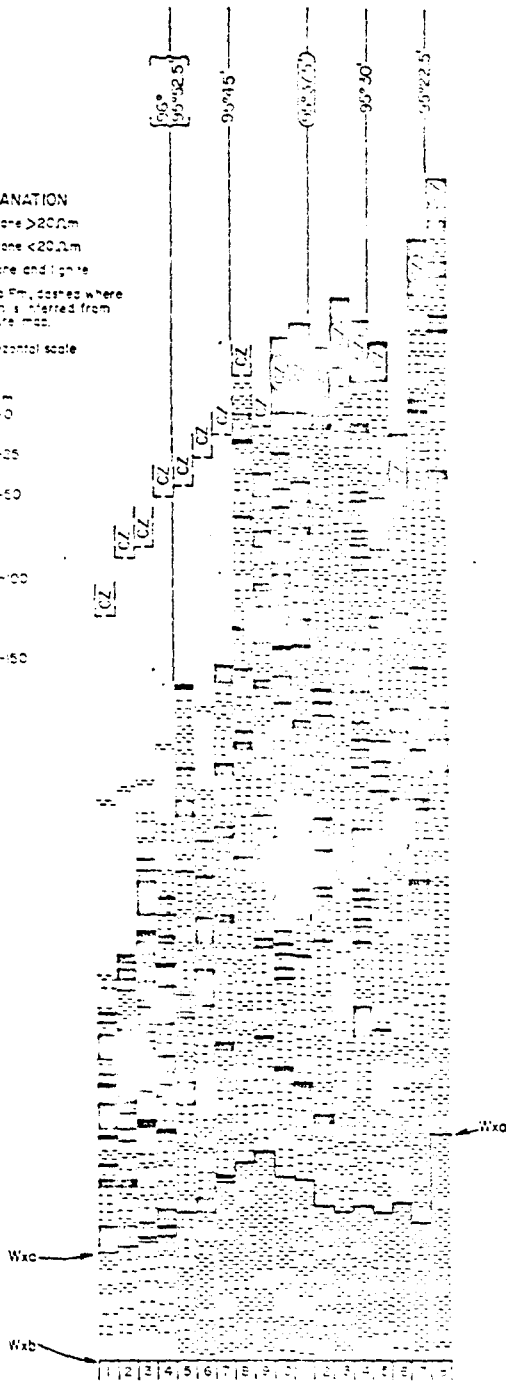
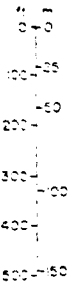
Variations in the response of ILD logs were reduced to three conditions: (1) "clean" sandstones with resistivities greater than  $20\ \underline{\mu}\text{m}$ , (2) "muddy" sandstones with resistivities less than  $20\ \underline{\mu}\text{m}$ , and (3) mudstones with resistivities generally less than  $10\ \underline{\mu}\text{m}$  and with a baseline SP.

Compressed cross sections are based on strip logs of the distribution of these three conditions through the Wilcox section. The horizontal datum for the compressed section is the top of the Midway because in many wells the upper part of the Wilcox is missing due to erosion or was not logged. The lateral spacing between strip logs was compressed until the logs were side-by-side. The compressed sections emphasize the lateral relationships and distribution of sandstones greater than  $20\ \underline{\mu}\text{m}$ . These relationships are apparent in figure \_\_, which shows the compressed sections in a fence diagram.



E (WEST) (EAST) E'

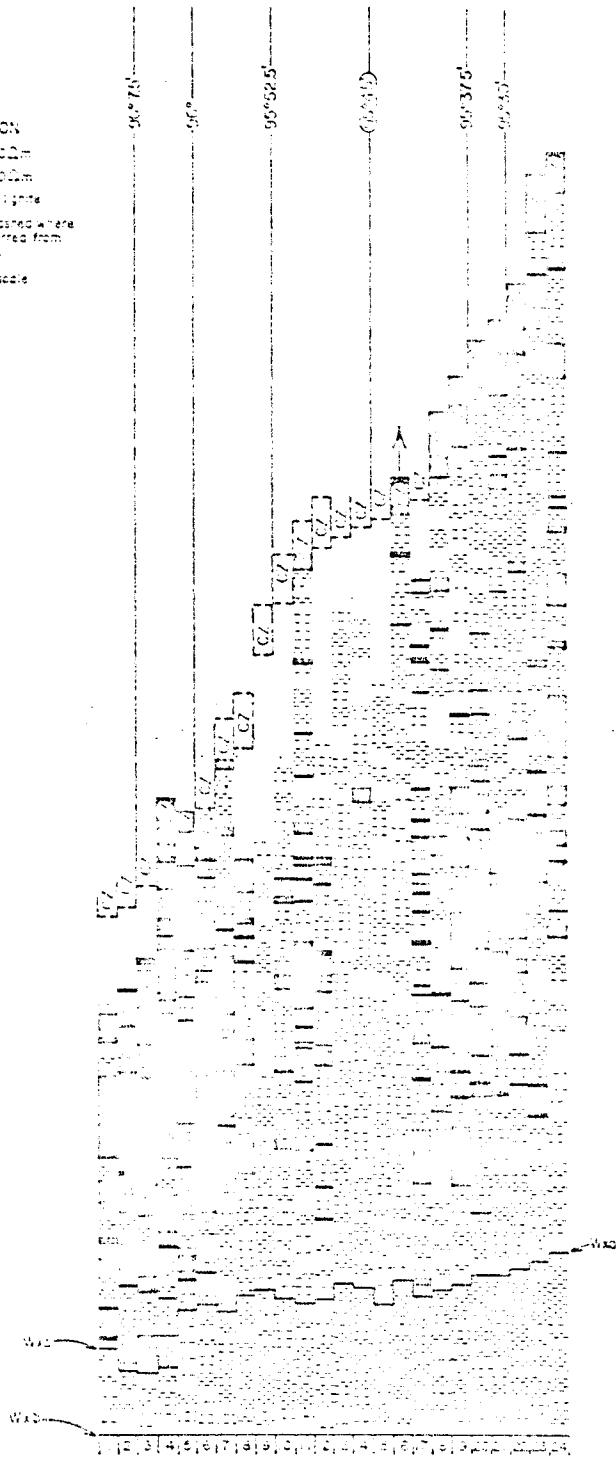
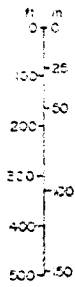
EXPLANATION  
Sandstone >200m  
Sandstone <200m  
Mudstone and lignite  
CZ Corozo Fm., dashed where position is inherited from structure map  
No horizontal scale



G (WEST)

(EAST) G'

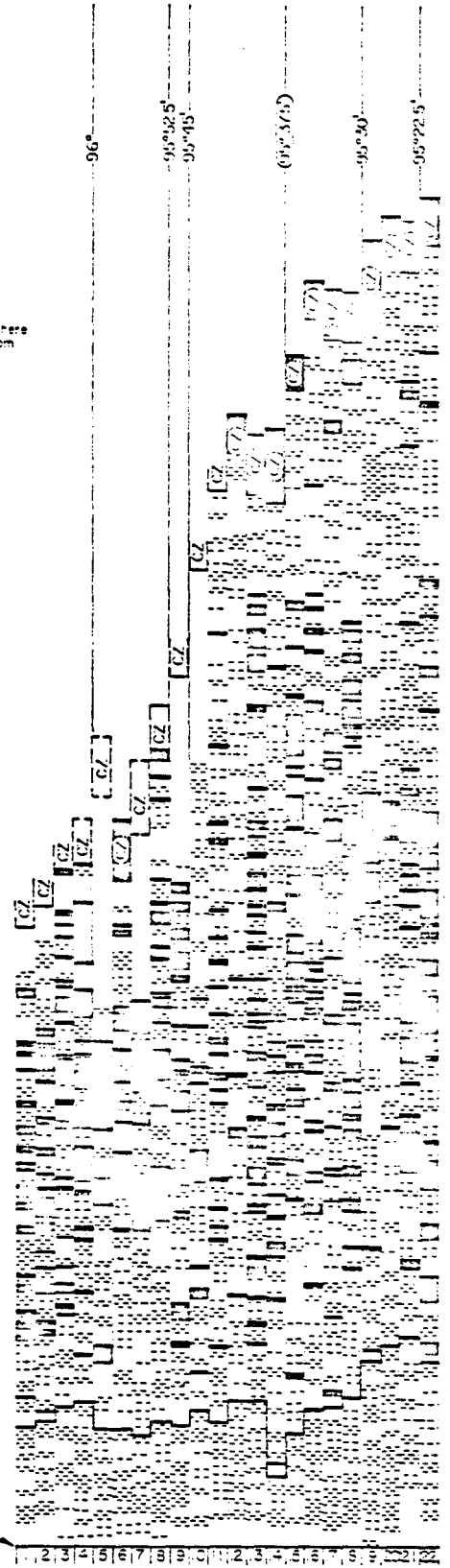
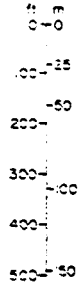
- EXPLANATION**
-  Sandstone > 200m
  -  Sandstone < 200m
  -  Mudstone and lignite
  - CZ** Corridor Pm, joined where position is inferred from structure map
- No horizontal scale



I (WEST)

(EAST) I'

- EXPLANATION**
-  Sandstone >200m
  -  Sandstone <200m
  -  Mudstone and lignite
  -  Corridors Emplaced where position is inferred from structure map
  - No horizontal scale



K(WEST)

(EAST)K'

EXPLANATION

-  Sandstone >200m
-  Sandstone <200m
-  Mudstone and shale
-  Same as the pattern where location is marked from structure into
-  In horizontal scale

0 0.5  
100 25  
200 50  
300 75  
400 100  
500 125

Wxa

Wxb

Wxa

1 2 3 4 5 6 7 8 9 10 11 12 13 14 15 16 17 18 19 20 21 22



M(WEST)

(EAST)M'

- EXPLANATION
-  Sandstone >200m
  -  Sandstone <200m
  -  Mudstone and shale
  -  Corralo Fm. located where position is inferred from structure map
  - No horizontal scale

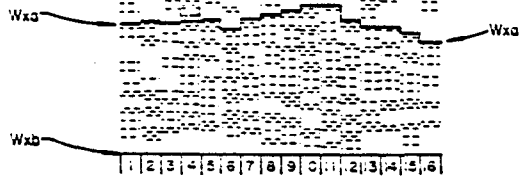
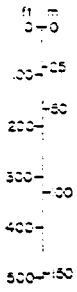


TABLE AND FIGURES

	Oakwood	Butler	Palestine	Keechi	Bethel	Boggy Creek	Brushy Creek	Concord	Ave.
Minimum depth to salt or cap rock m (ft)	214 (703)	95 (312)	37 (120)	38 (125)	430 (1411)	683 (2242)	889 (2916)	<del>1830</del> (6000)	
Wilcox in contact with dome	yes	no?	yes	yes	yes	no	no	no	
Percentage thinning	13	nearly complete piercement-uplift overdome <i>space</i>	nearly complete piercement-uplift overdome <i>space</i>	nearly complete piercement-uplift overdome <i>space</i>	40	12	46	1	
Percentage thickening	22	8	8	47	35	33	23	1	22%
Near-dome facies change	yes	yes	yes	yes	yes	maybe	no	no	

Table 1

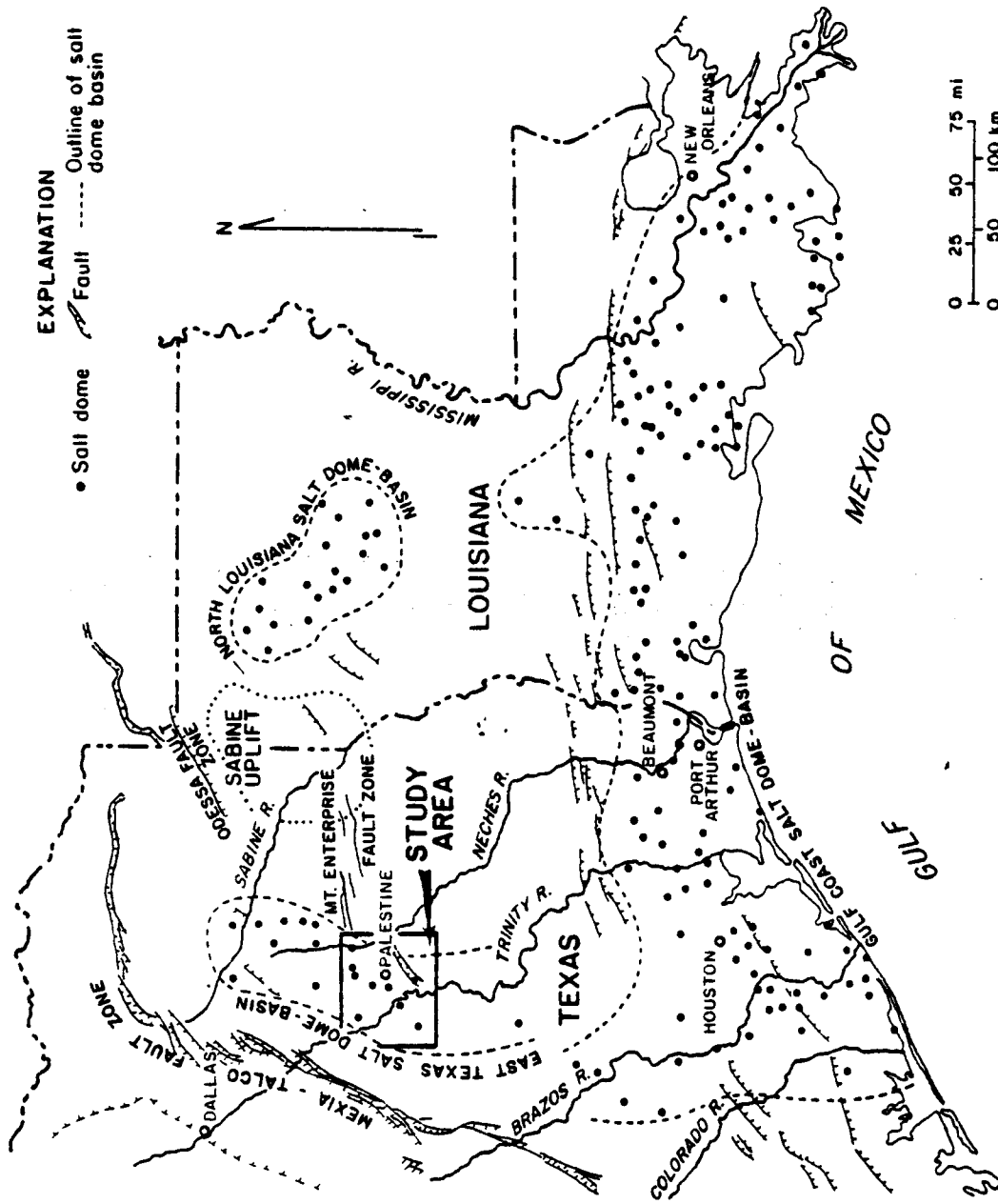


Fig 1



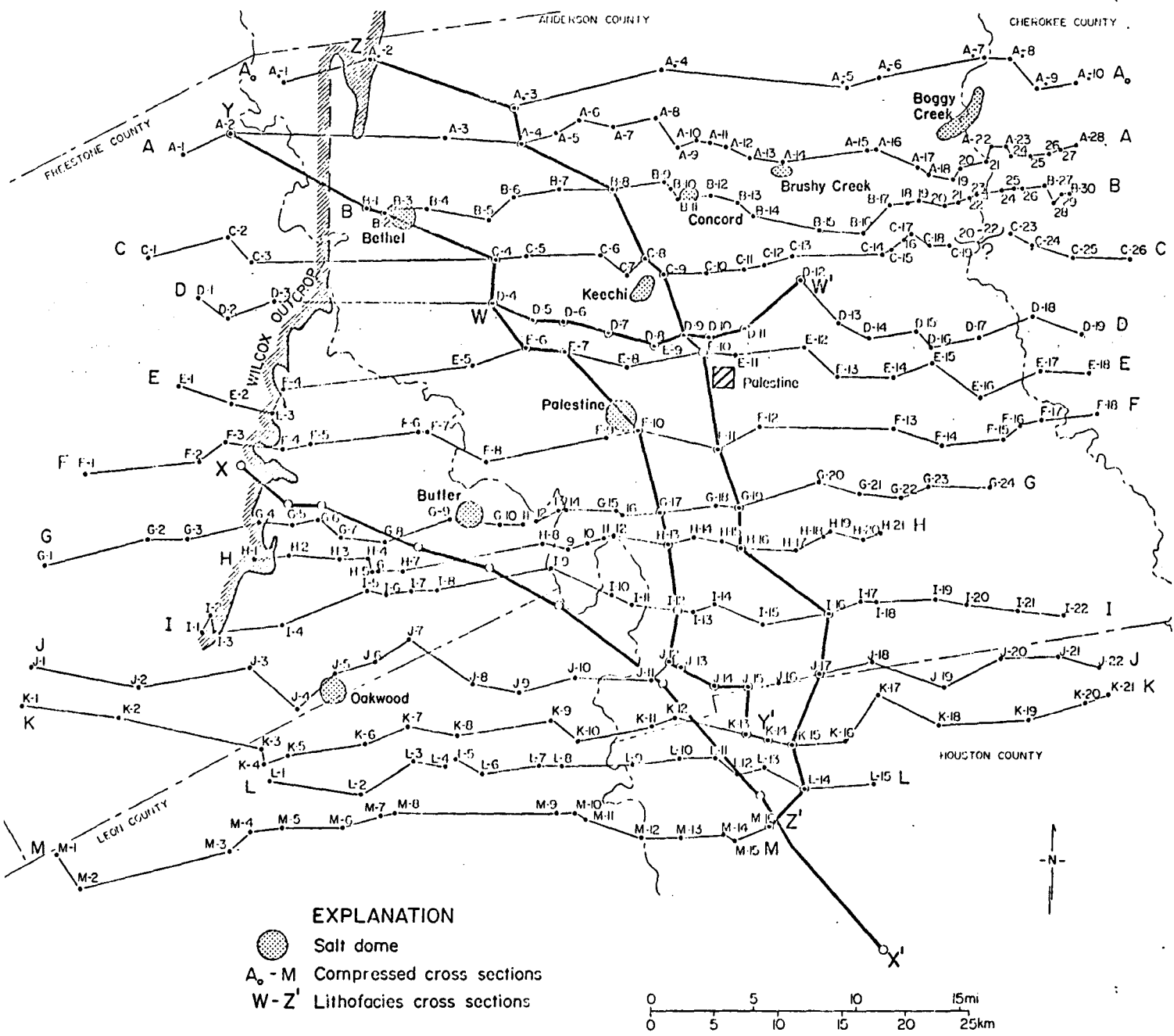


Fig 3

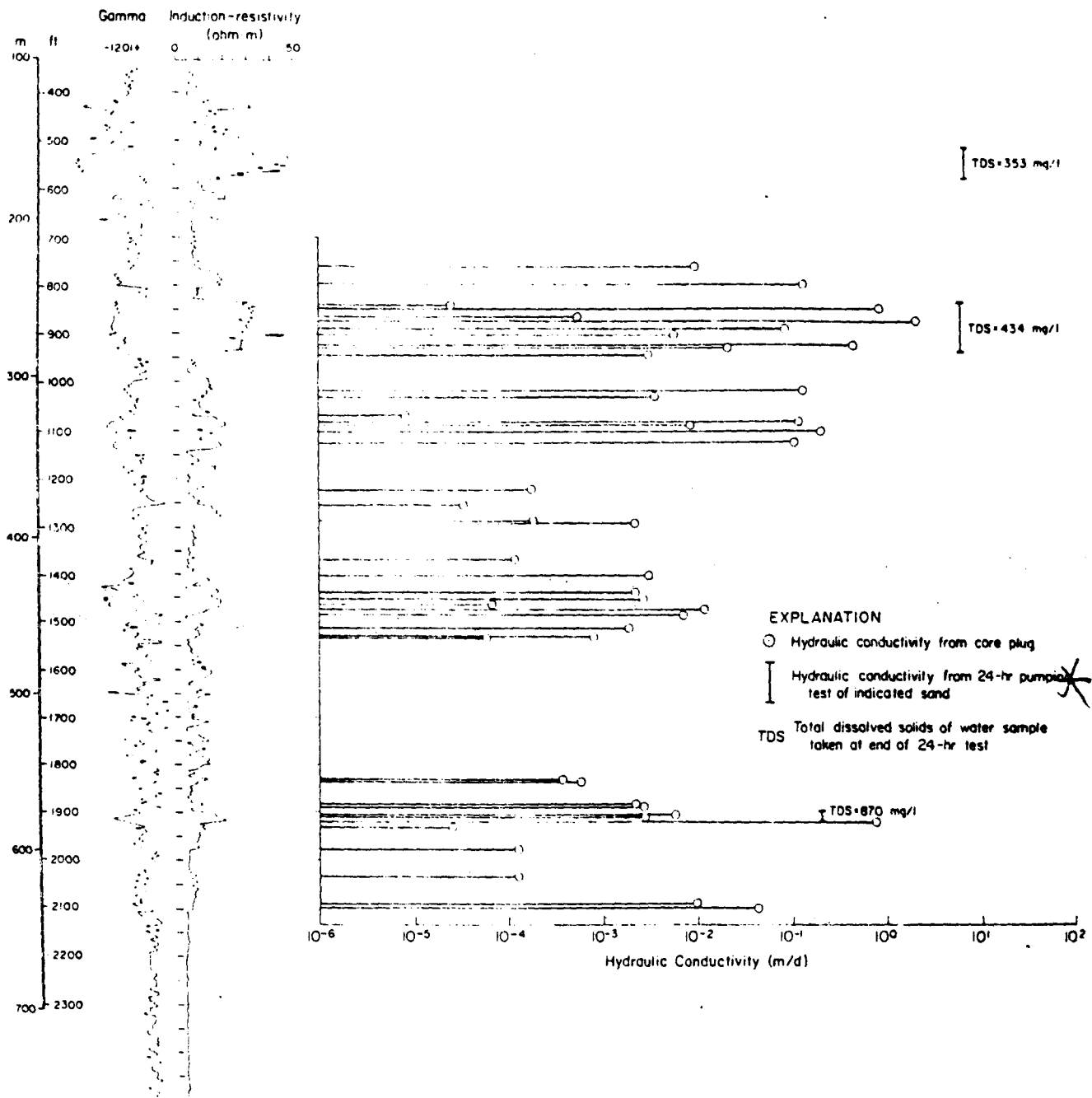
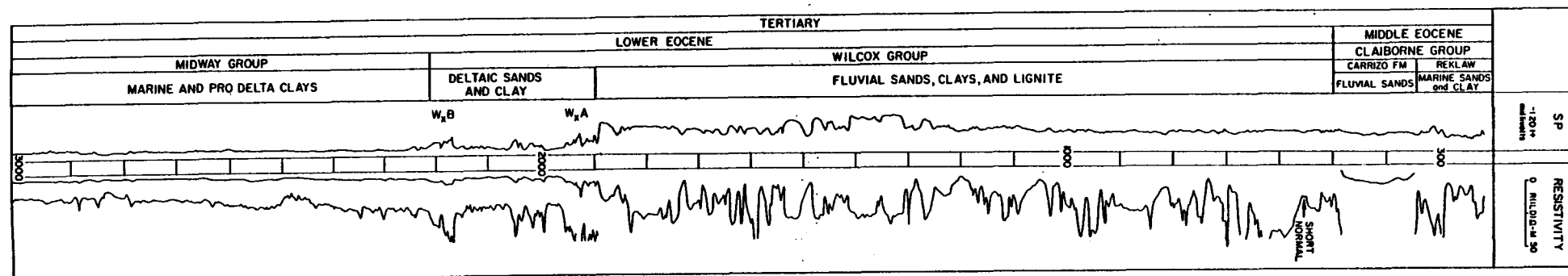


Fig 4



F15



Fig 6

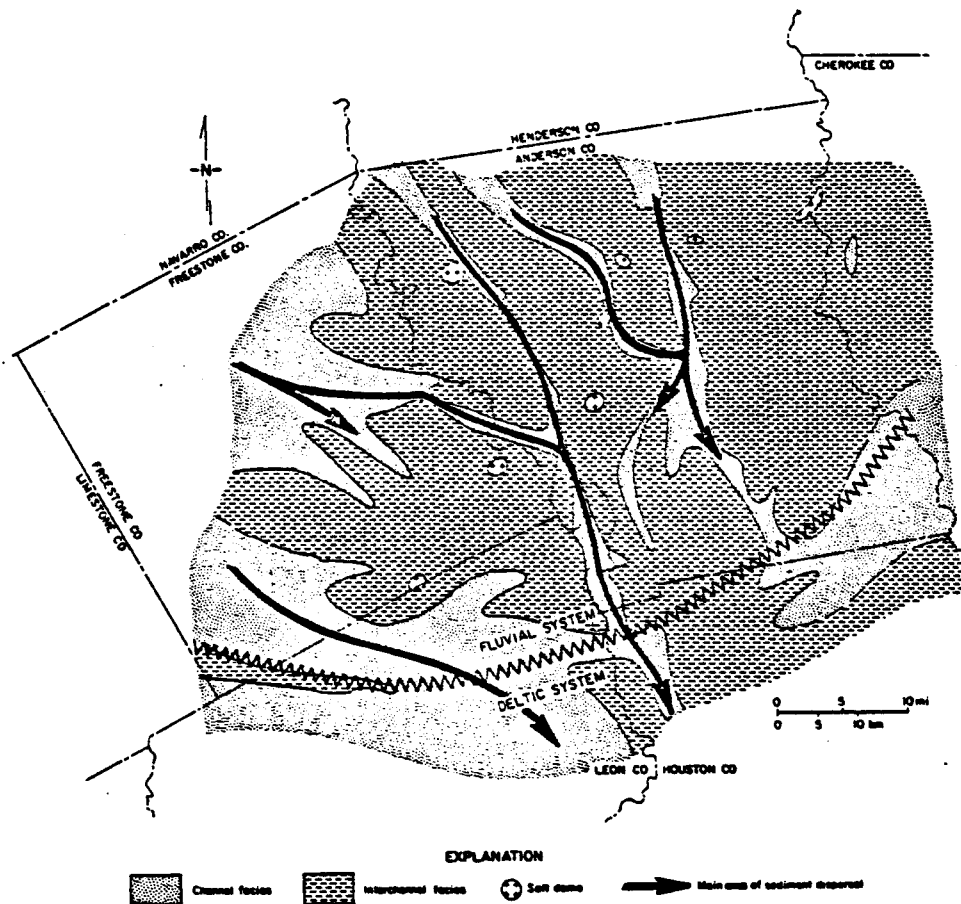


Fig 7

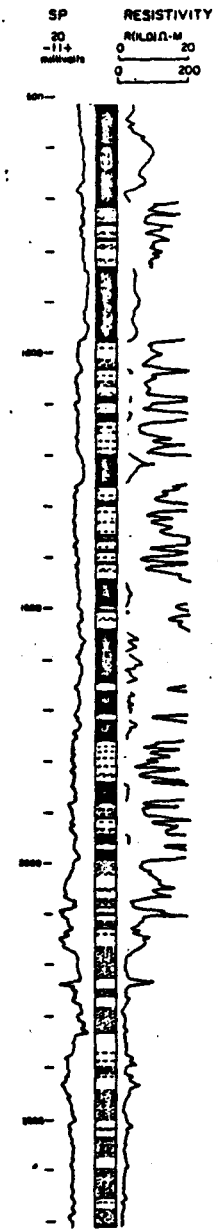
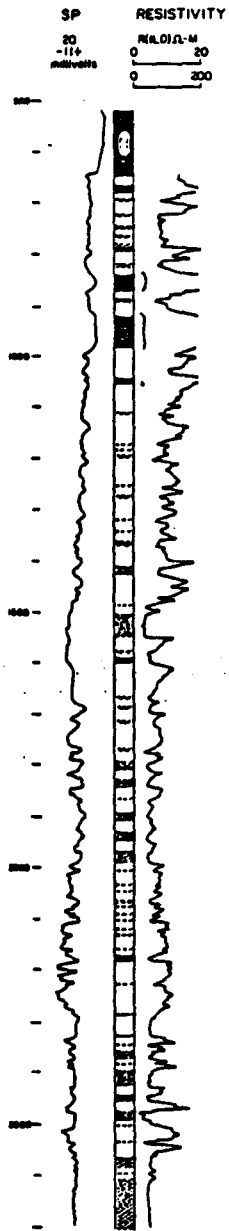


Fig 8

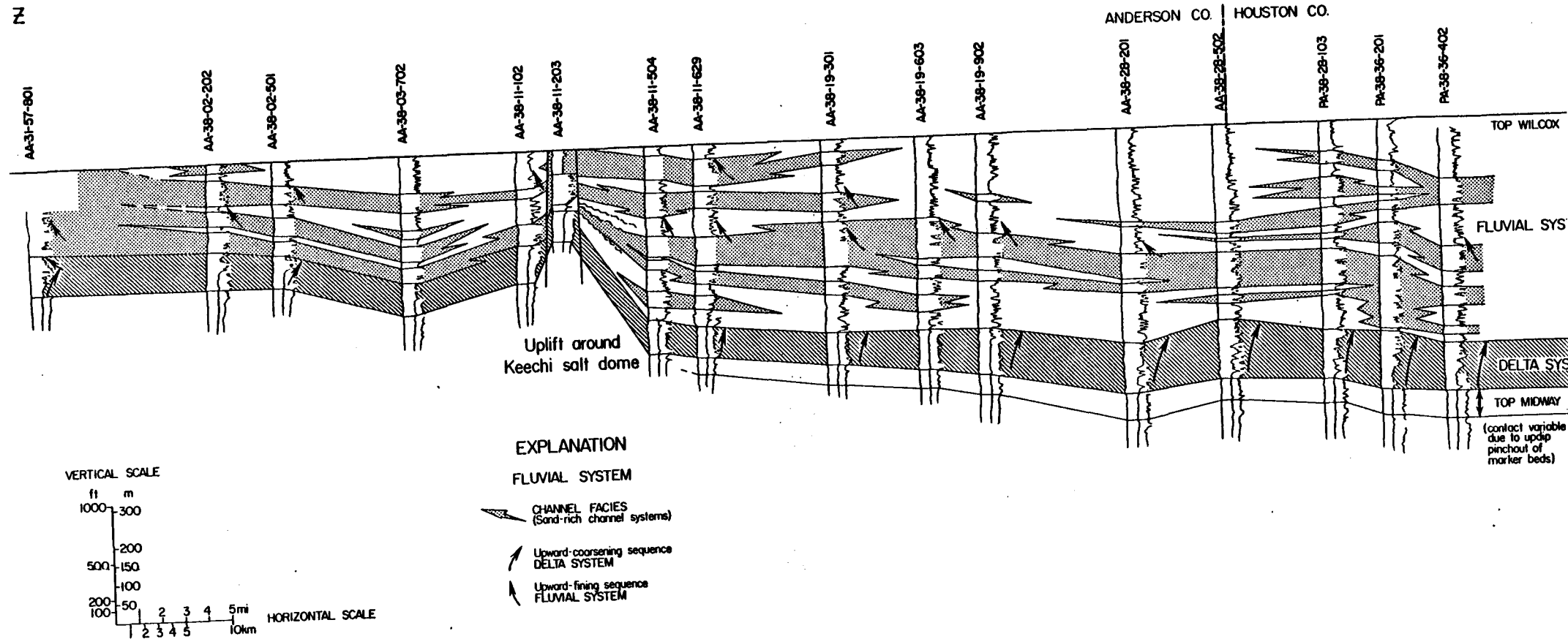


Fig 9

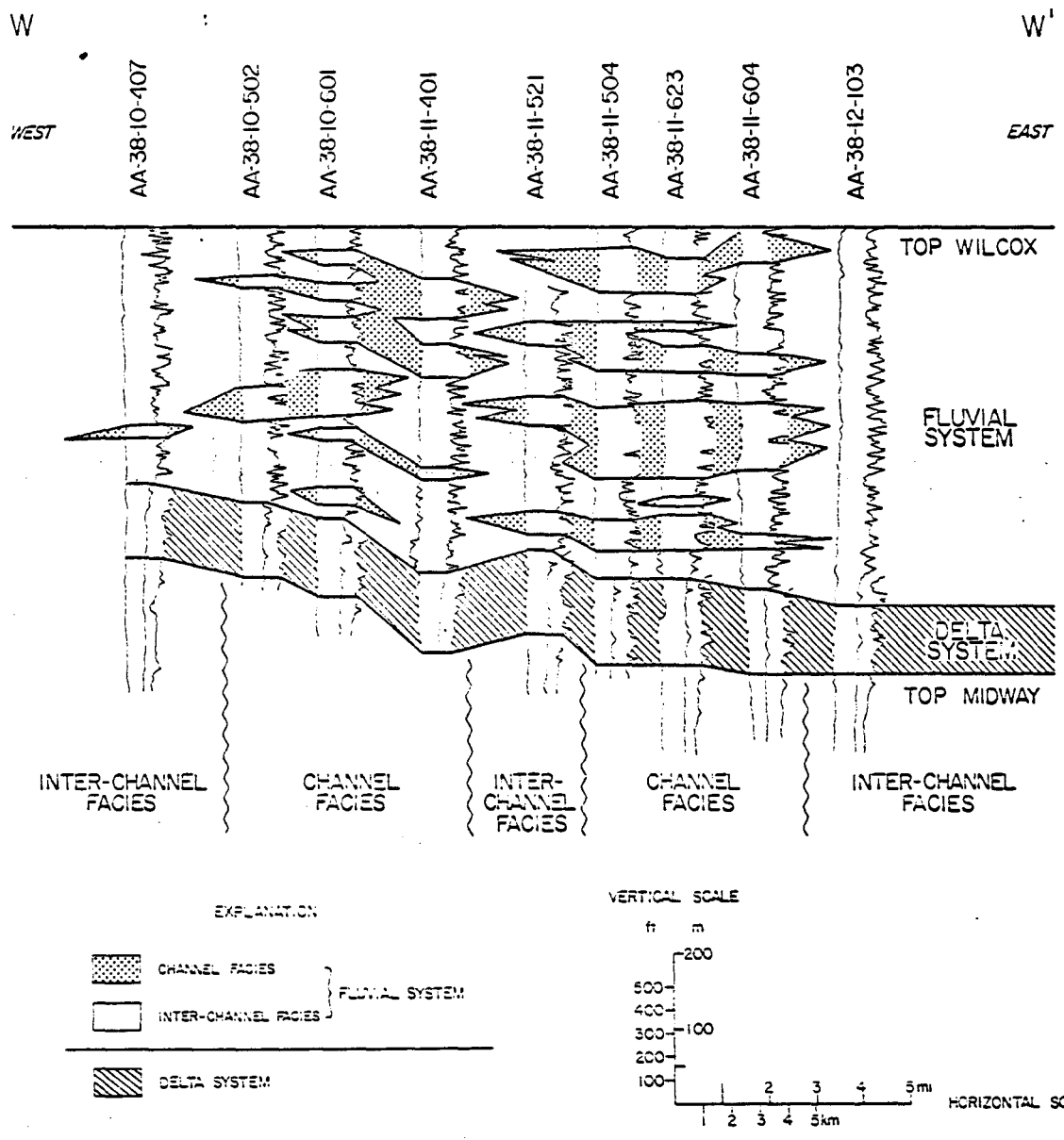


Fig 10

TOH-2A  
CHANNEL LAG



Depth 950'  cm/in.  
SCALE

Fig 11

SP RESISTIVITY  
20  
10  
0  
-10  
-20  
M.A.D.D.-M  
0 20  
200

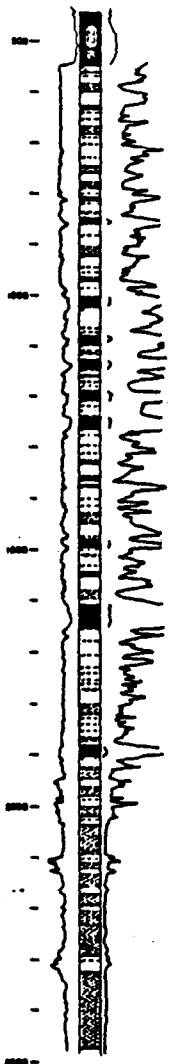


Fig 12

V

100  
100  
100

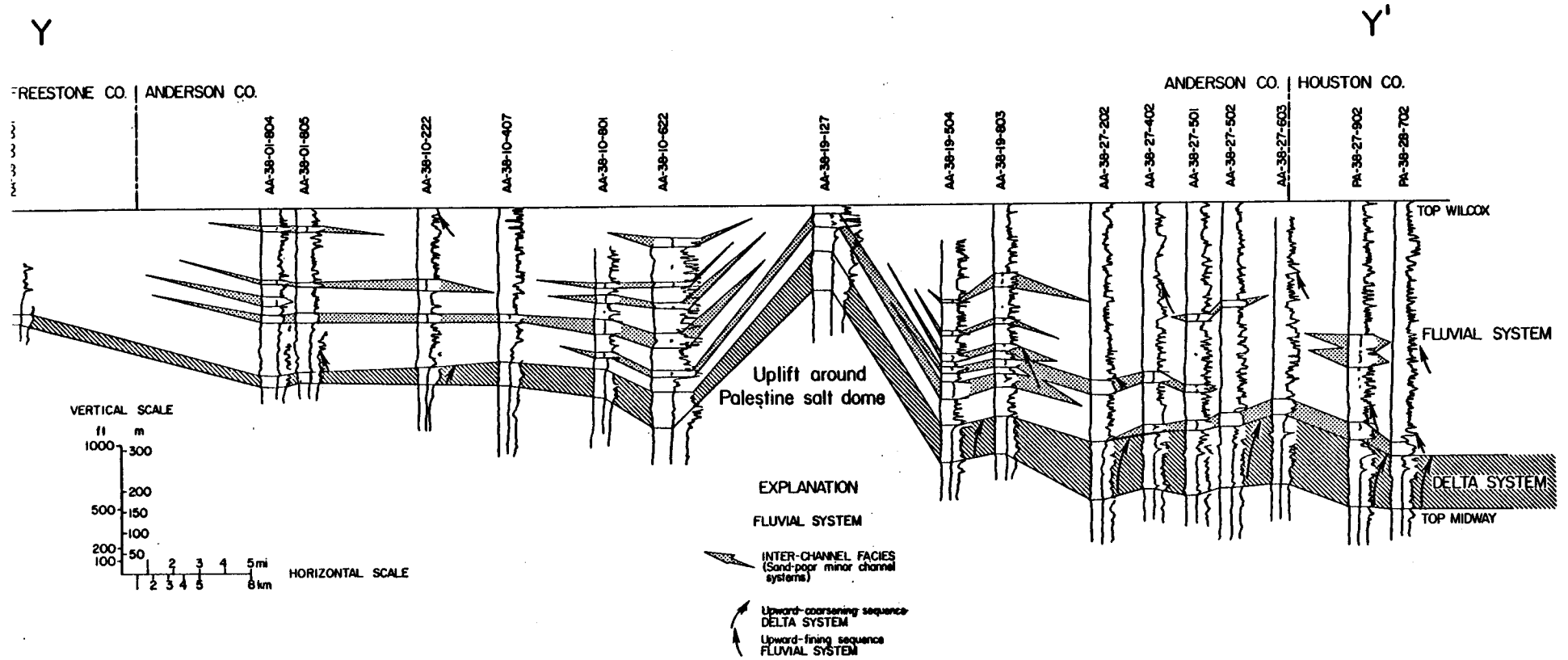
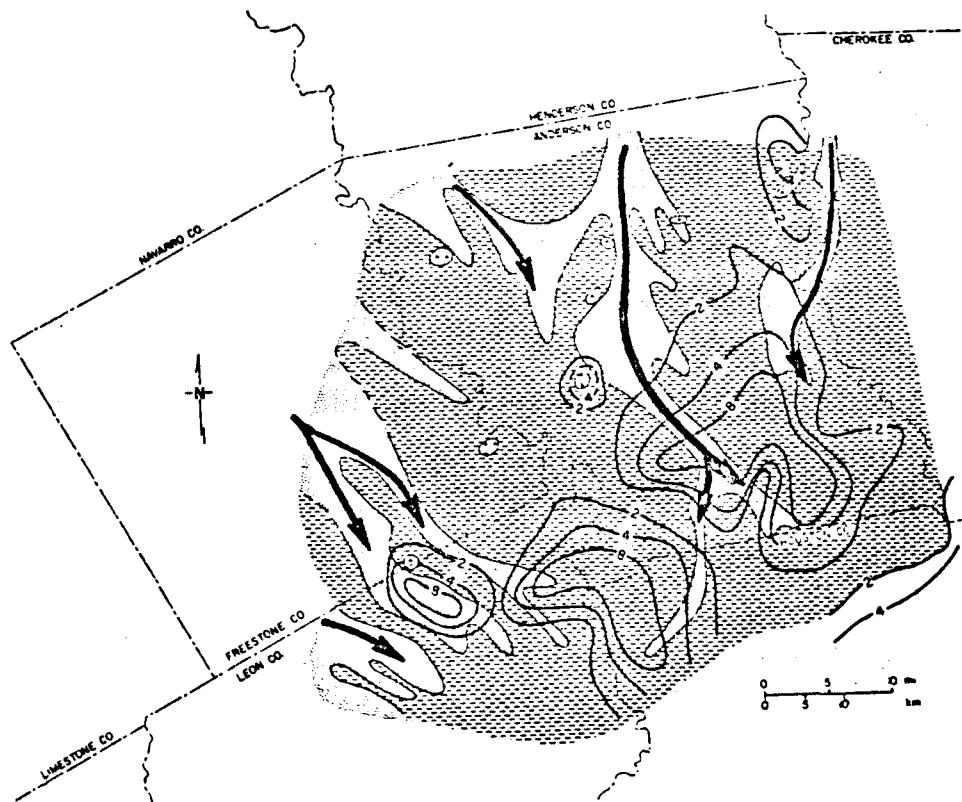


Fig 13



EXPLANATION

-  Channel facies
  -  Interchannel facies
  -  Number of light beds after Kaiser (1974)
  -  Salt dome
-  Main axes of sediment dispersal

- Galloway, W. E., 1968, Depositional systems of the lower Wilcox Group, North-Central Gulf Coast Basin: Gulf Coast Assn. of Geological Societies Trans., v. 18, p. 275-289.
- Galloway, W. E., 1977, Catahoula Formation of the Texas Coastal Plain: depositional systems, composition, structural development, groundwater flow history and uranium distribution: The University of Texas, Bureau of Economic Geology, Report of Investigations No. 87, 59 p.
- Galloway, W. E., and Kaiser, W. R., 1980, Catahoula Formation of the Texas Coastal Plain: Origin, geochemical evolution and characteristics of uranium deposits: The University of Texas, Bureau of Economic Geology, Report of Investigations No. 100, 81 p.
- Giles, A. B., 1980, Evolution of East Texas salt domes: in Kreitler, C. W., Agagu, O. K., Basciano, J. M., Collins, E. W., Dix, O., Dutton, S. P., Fogg, G. E., Giles, A. B., Guevara, E. H., Harris, D. W., Hobday, D. K., McGowen, M. K., Pass, D., and Wood, D. H., 1980, Geology and geohydrology of the East Texas Basin, a report on the progress of nuclear waste isolation feasibility studies (1979): The University of Texas at Austin Bureau of Economic Geology, Geological Circular 80-12, p. 20-29.
- Henry, C. D., and Basciano, J. M., 1979, Environmental geology of the Wilcox Group lignite belt, East Texas: The University of Texas, Bureau of Economic Geology, Report of Investigations 98, 28 p.
- Jones, L., 1977, Slice technique applied to uranium favorability in uppermost Tertiary of East Texas and West Louisiana: Gulf Coast Association of Geol. Soc. 27th Annual Meeting, p. 61-68.

- Kupfer, D. H., 1970, Mechanism of intrusion of Gulf Coast salt, in Geology and Technology of Gulf Coast Salt, a symposium: School of Geoscience, Louisiana State University, p. 25-66.
- Loocke, J. E., 1978, Growth history of Hainesville Salt Dome, Wood County, Texas: Unpub. Master's Thesis, The University of Texas at Austin, 95 p.
- McGowen, J. H., Brown, L. F., Jr., Evans, T. J., Fisher, 1976, Environmental geological atlas of the Texas Coastal Freeport area, The University of Texas at Austin, Environmental Geology, 98 p.
- Nettleton, L. L., 1934, Fluid mechanics of salt domes: American Association Petroleum Geologists Bulletin, v. 18, p. 1175-1204.
- Trusheim, F., Mechanism of salt migration in northern Germany: American Association Petroleum Geologists Bulletin, v. 44, p. 1519-1540.
- Toth, J., 1972, Properties and manifestations of regional ground-water movements: International Geological Congress, 24th, 1972, Proceedings, p. 153-163.
- Woodbury, H. O., Murray, I. B., Picford, P. J., and Akers, W. H., 1973, Pliocene and Pleistocene depocenters, outer continental shelf, Louisiana and Texas: Am. Assoc. Petroleum Geologists Bull., v. 57, no. 12, p. 2428-2439.

SP

Res

SP

Res

Carrizo Formation

KA-39-25-501

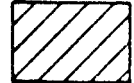
Carrizo Formation

Carrizo Formation

Fluvial Facies



Fluvial facies



Deltaic facies



Ground-anomaly



Upward sequence

ft

500

400

300

200

100

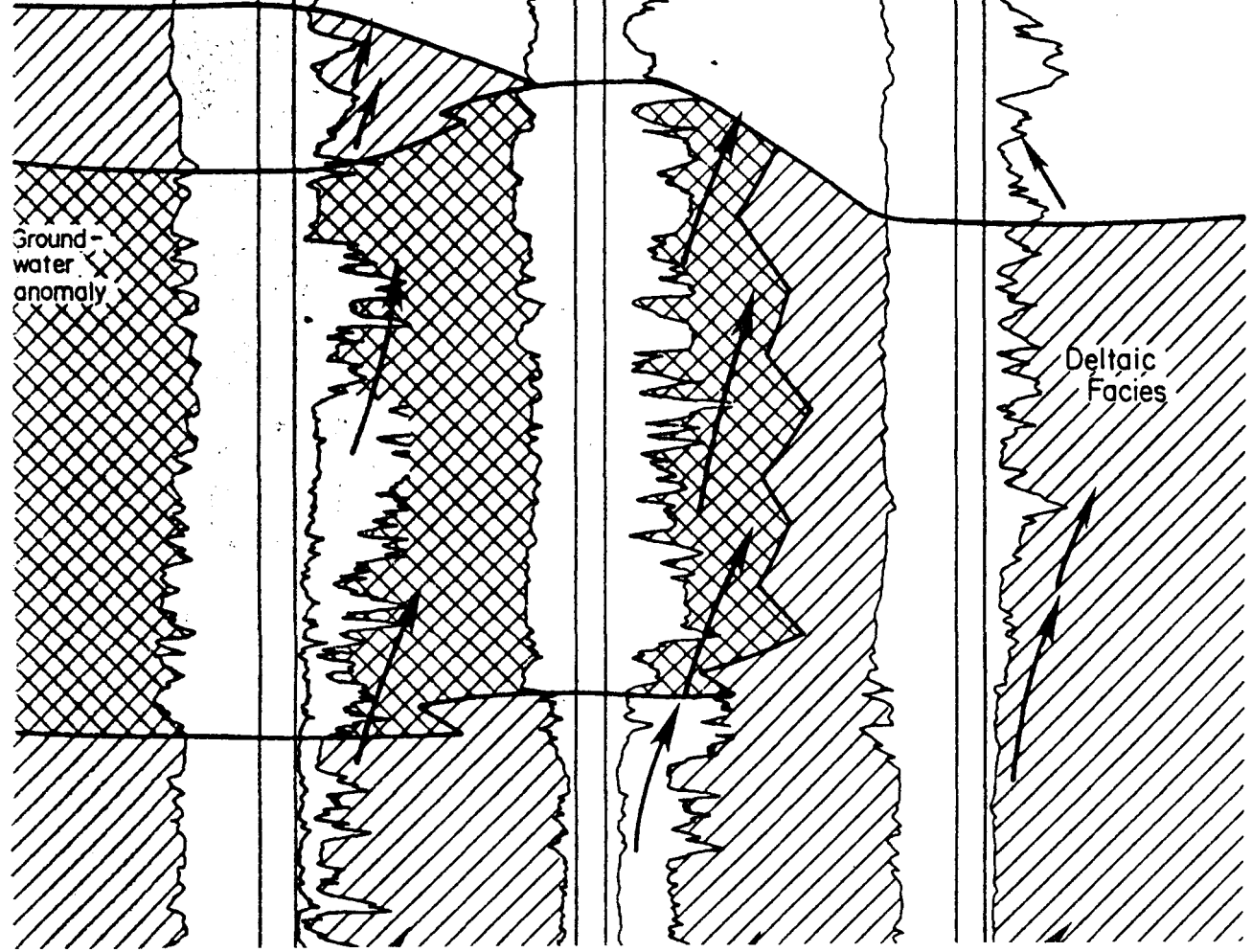
0

Verti

No hor

Ground-water anomaly

Deltaic Facies



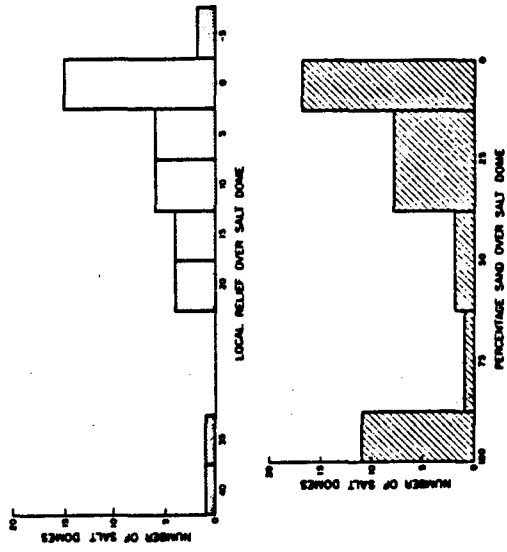
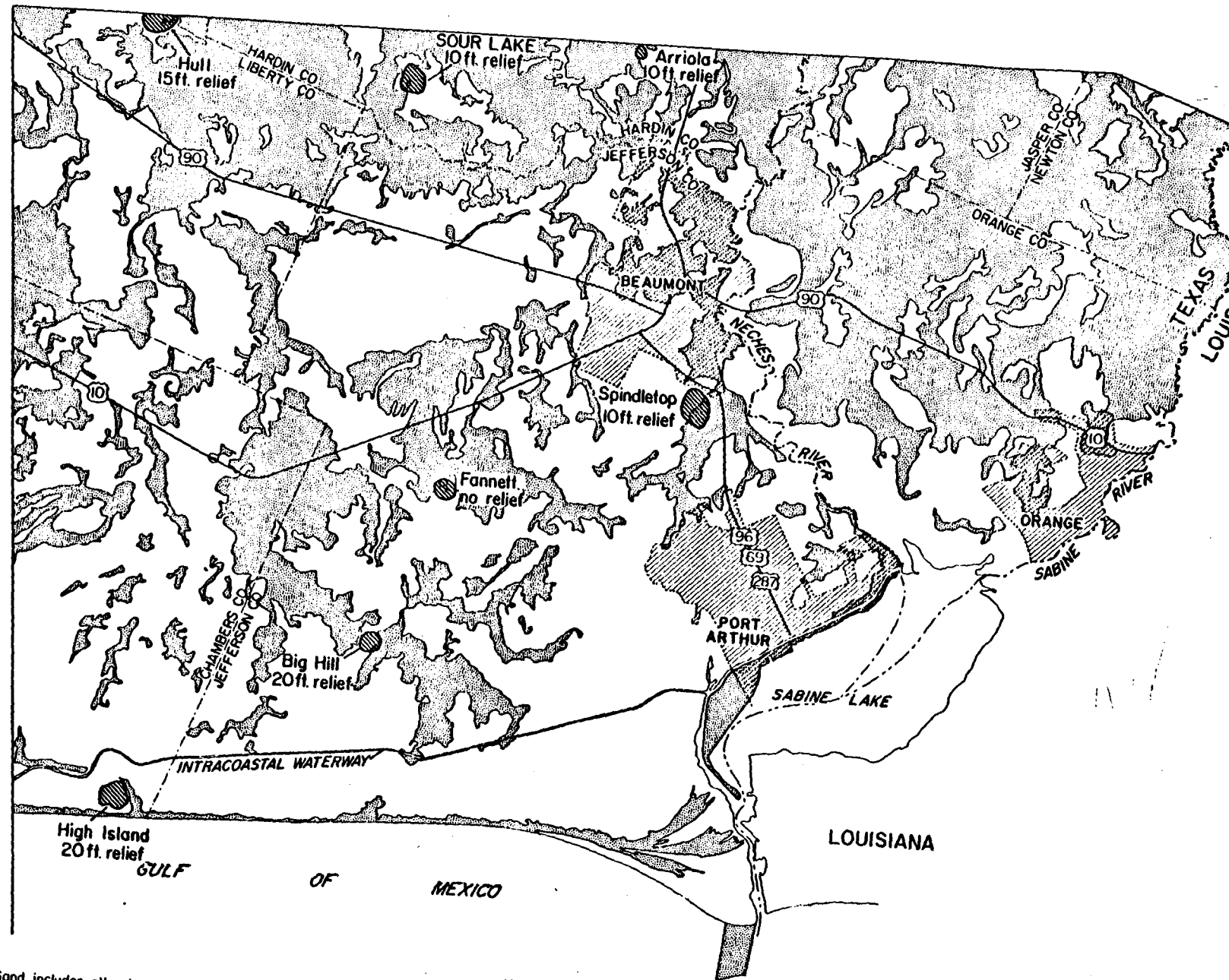


Fig 18



Sand, includes all subaerial sandy deposits, fluvial sand, distributary sand and silt with local mud, strandplain-chenier sand, and subaqueous-subaerial spoil

**EXPLANATION**

Mud, includes all subaerial muddy deposits, floodbasin mud, interdistributary mud, marsh and swamp facies, mud-filled strandplain-chenier swales, mud-flats

Salt dome, shallow piercement, projected outline (approximate) of dome, some surface expression, with local relief in feet

Fig 19

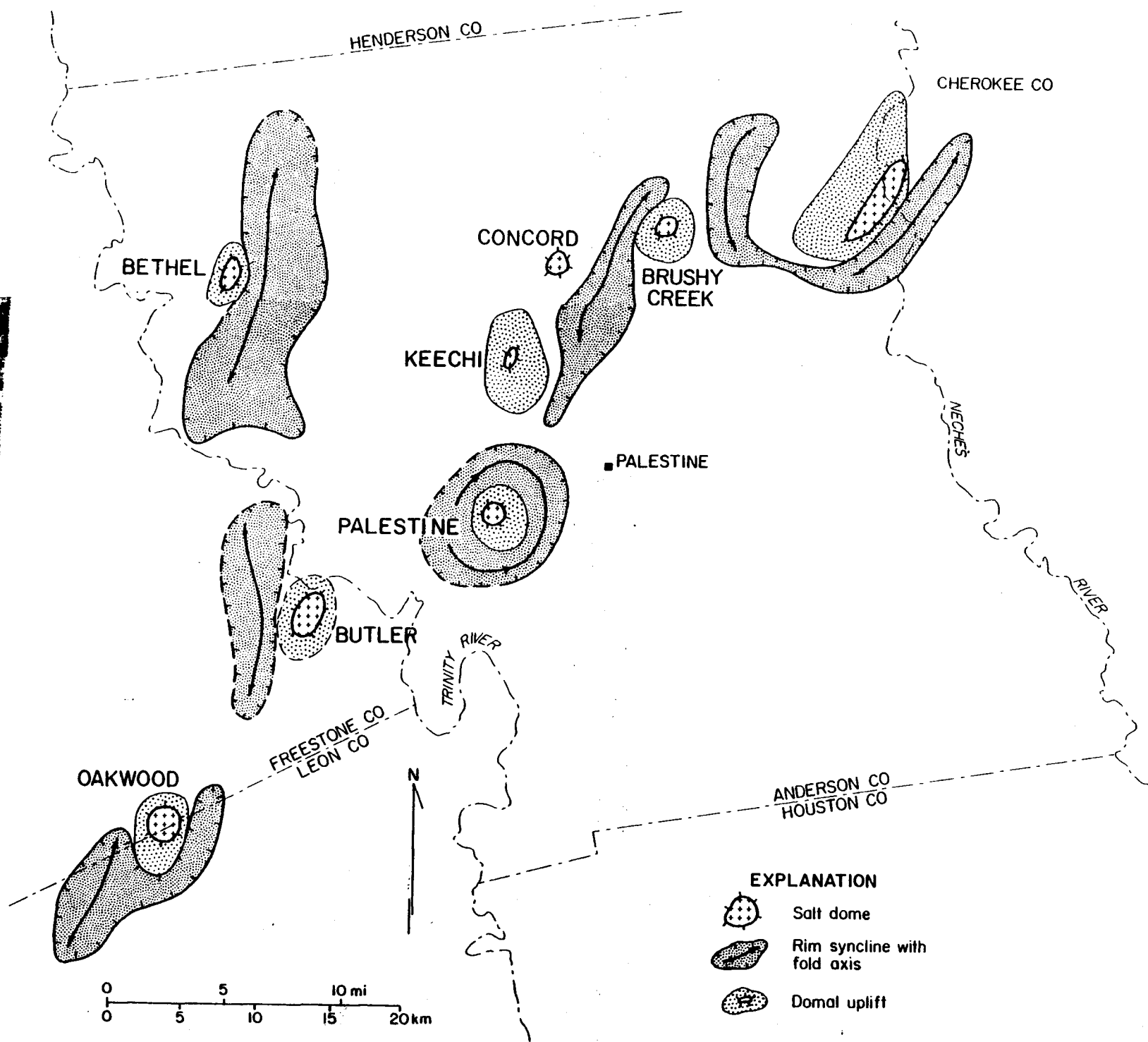
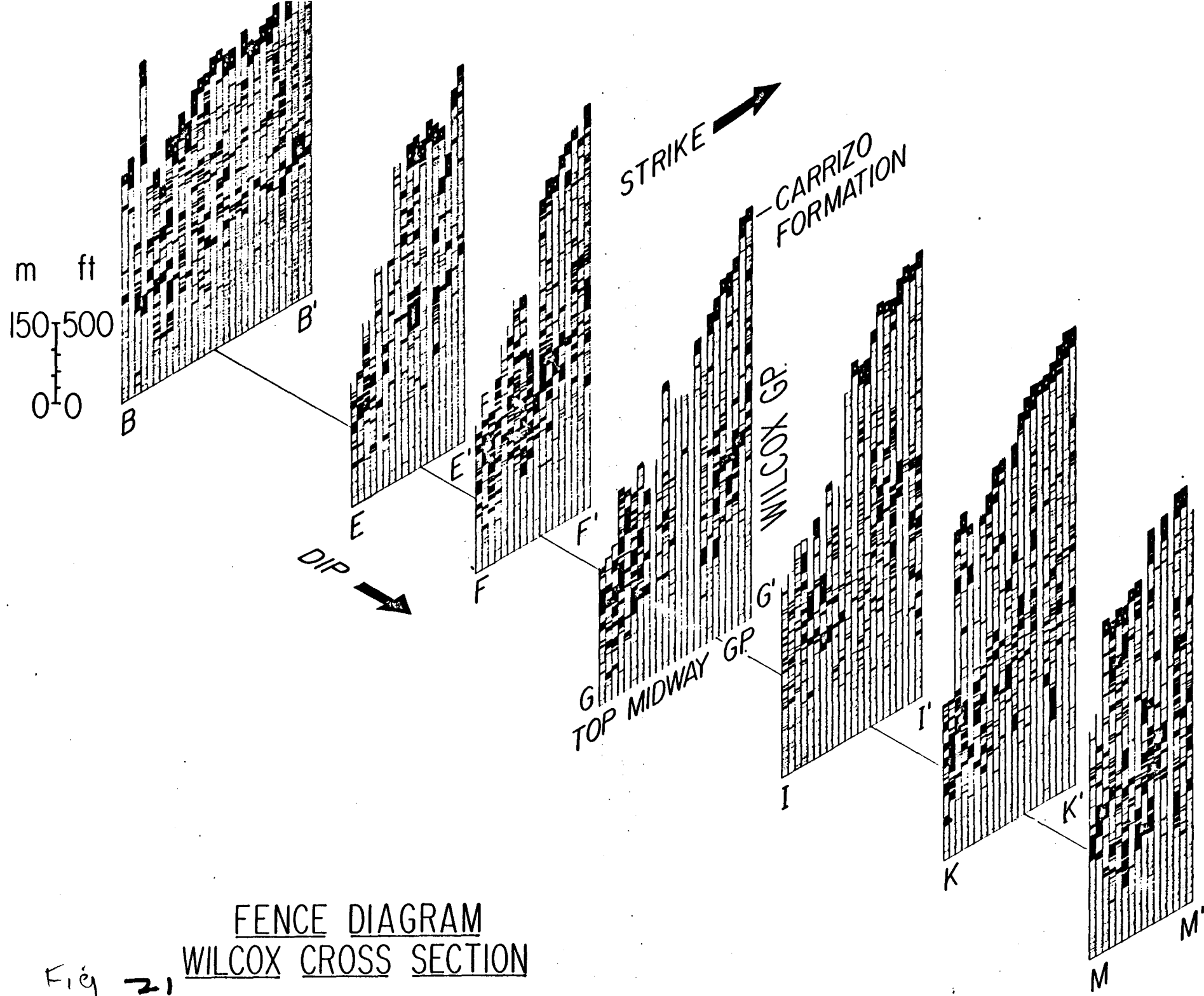


Fig 20



FENCE DIAGRAM  
WILCOX CROSS SECTION

Fig 21  
M

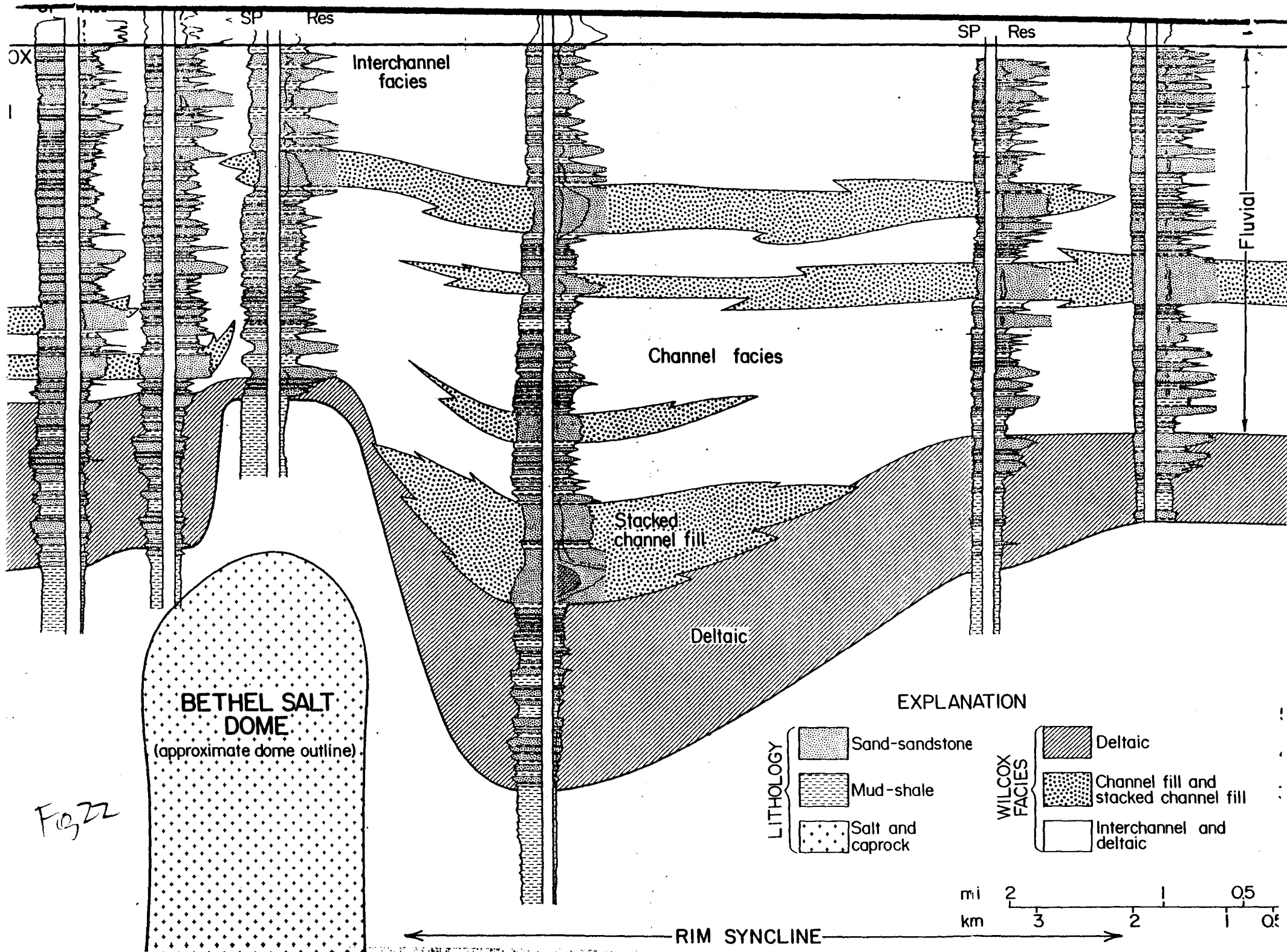


Fig 22

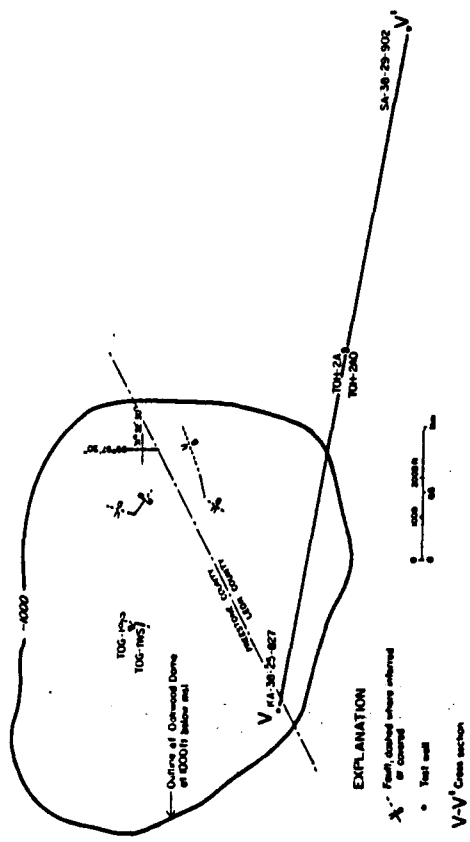
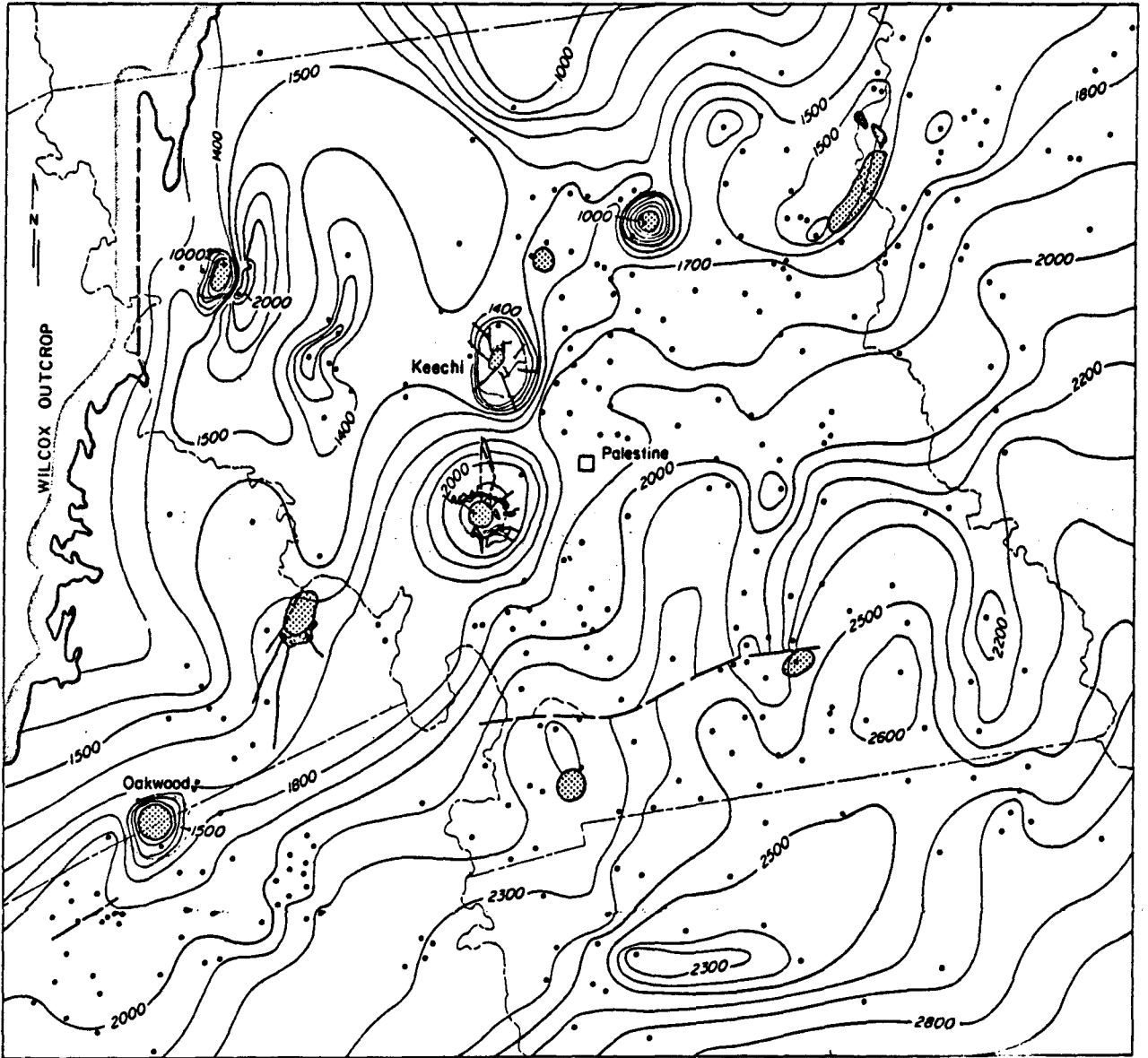


Fig 23  
S



Outcrop of Wilcox Group    
  Salt dome    
  Fault at mapped horizon    
 Contour interval: 100 ft. Datum: sea level

Fig 24

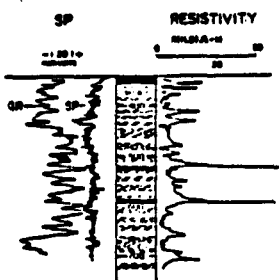
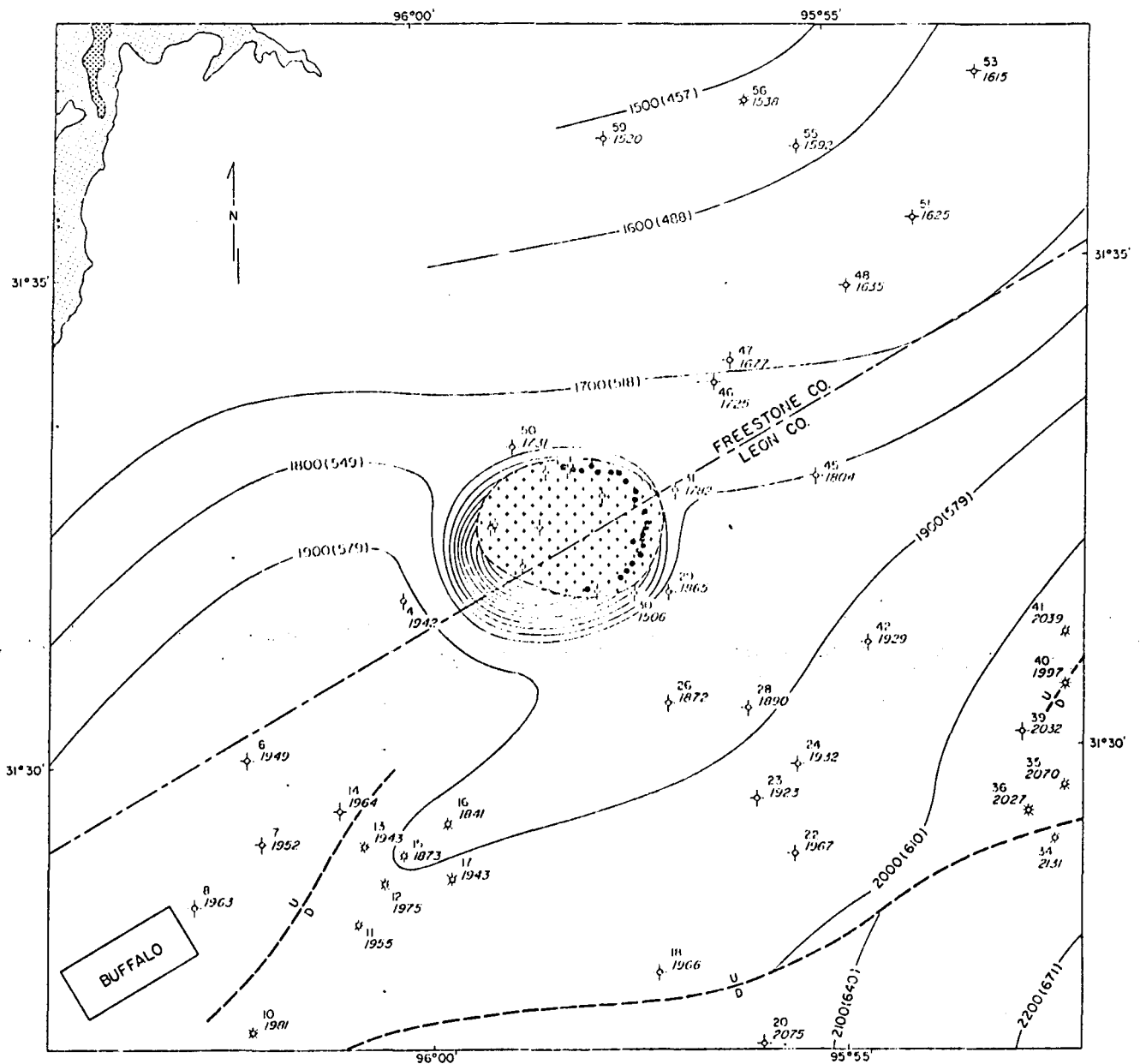


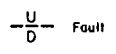
Fig. 25



1900(579) Isochore - Wilcox Group  
 Thickness in ft (m)  
 C.I. = 100 ft (30.5 m)

 Approximate dome area

 Dry well  
 Oil well  
 Gas well

 Fault

 Quaternary alluvium  
 Outcrop of Wilcox sediments

0 1 2 3 mi  
 0 1 2 3 km

Fig.  
 26  
 D

SW

NE

SANDSTONE GREATER THAN 20  $\Omega \cdot m$

-  > 200'
-  100' - 200'
-  50' - 100'
-  < 50'
-  SALT

DATUM

TOP OF WILCOX

1/3 WILCOX UPPER LAYER

1/3 WILCOX MIDDLE LAYER

1/3 WILCOX LOWER LAYER

BASE OF WILCOX

OAKWOOD SALT DOME

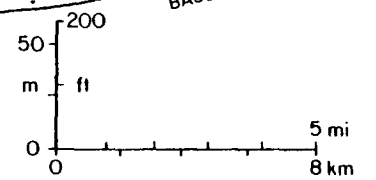


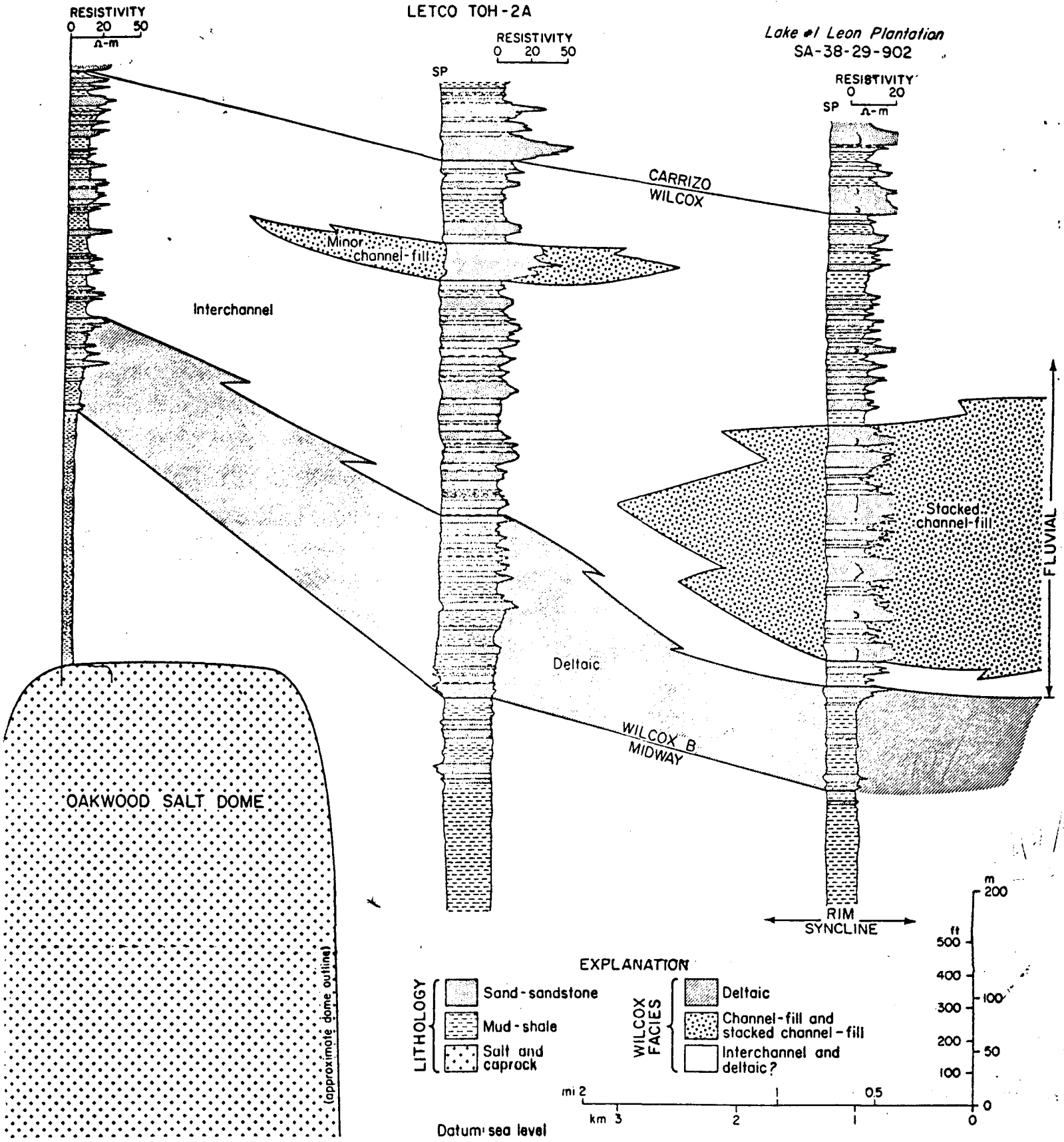
Fig 27



V  
NW  
McBee #1 M-Storms  
KA-38-25-827

V  
SE  
Lake #1 Leon Plantation  
SA-38-29-902

LETCO TOH-2A



8 Fig. 28